

Giornata Seminariale REFRESCOS

Dip. di Ingegneria Strutturale e Geotecnica – Politecnico di Torino, Italy

Luglio 1, 2010

**Emissione di energia dalla frattura di provini in
compressione: Acustica, elettromagnetica,
piezonucleare**

Alberto Carpinteri

Department of Structural Engineering and Geotechnics, Politecnico di Torino, Italy



ACKNOWLEDGEMENTS

Dr. Giuseppe Lacidogna (Politecnico di Torino);

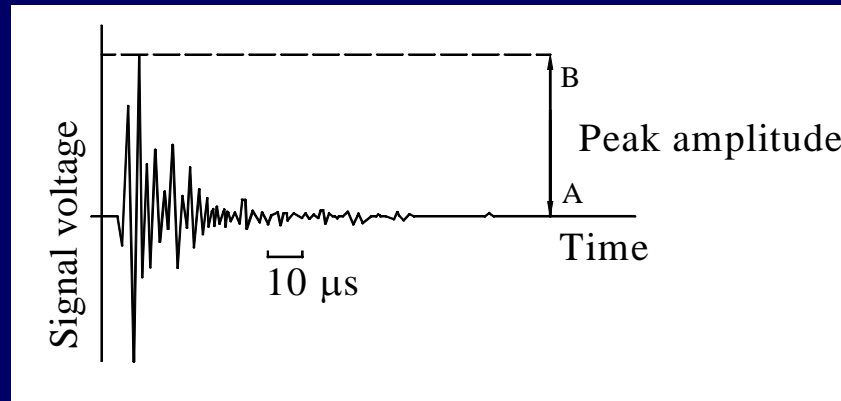
Dr. Amedeo Manuello (Politecnico di Torino);

Dr. Gianni Niccolini (National Research Institute of Metrology, INRIM);

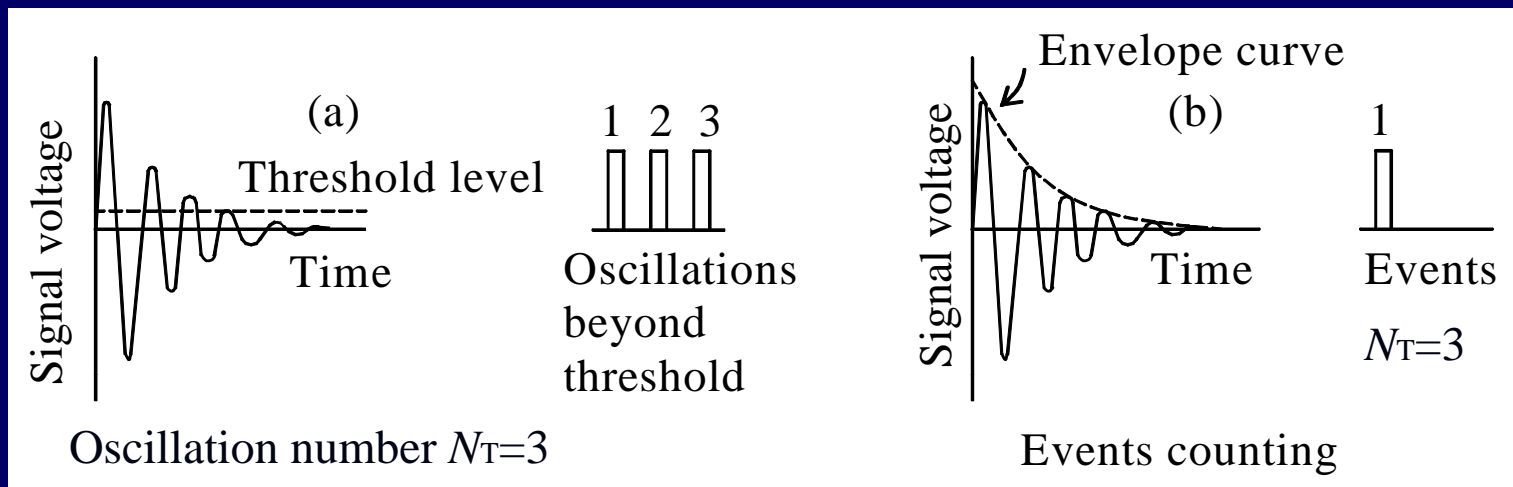
Dr. Fabio Cardone (National Research Council, CNR);

Dr. Oscar Borla (National Institute of Nuclear Physics, INFN).

AE signal identified by sensor



AE counting method



- The event intensity is measured by the oscillation number N_T
- The oscillation number N_T increases with the signal amplitude

FRACTAL SCALING OF ACOUSTIC EMISSION

Recently AE data have been interpreted on the basis of the statistical and fractal theories of fragmentation (*).

The following *size-scaling law* can be considered:

$$W \propto N \propto V^{D/3}, \quad (1)$$

W: released energy;

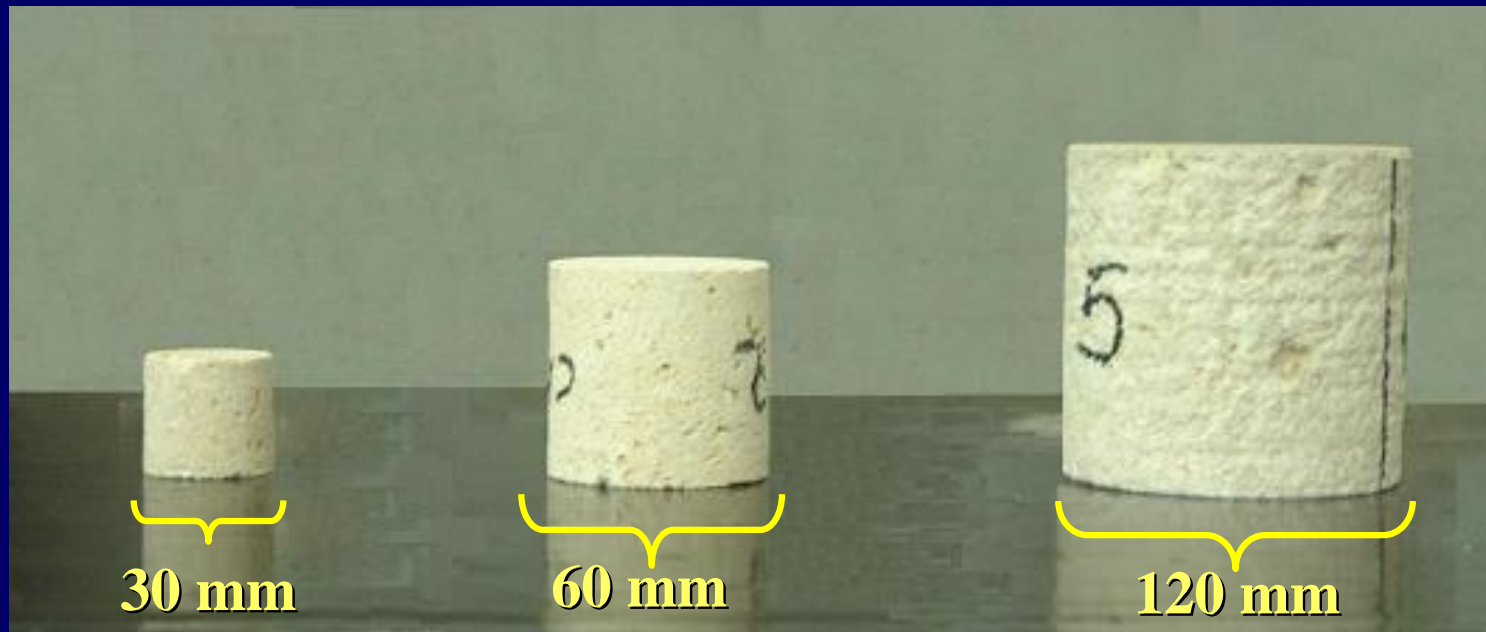
N: cumulative number of AE events that the structure provides during damage monitoring;

V: specimen volume;

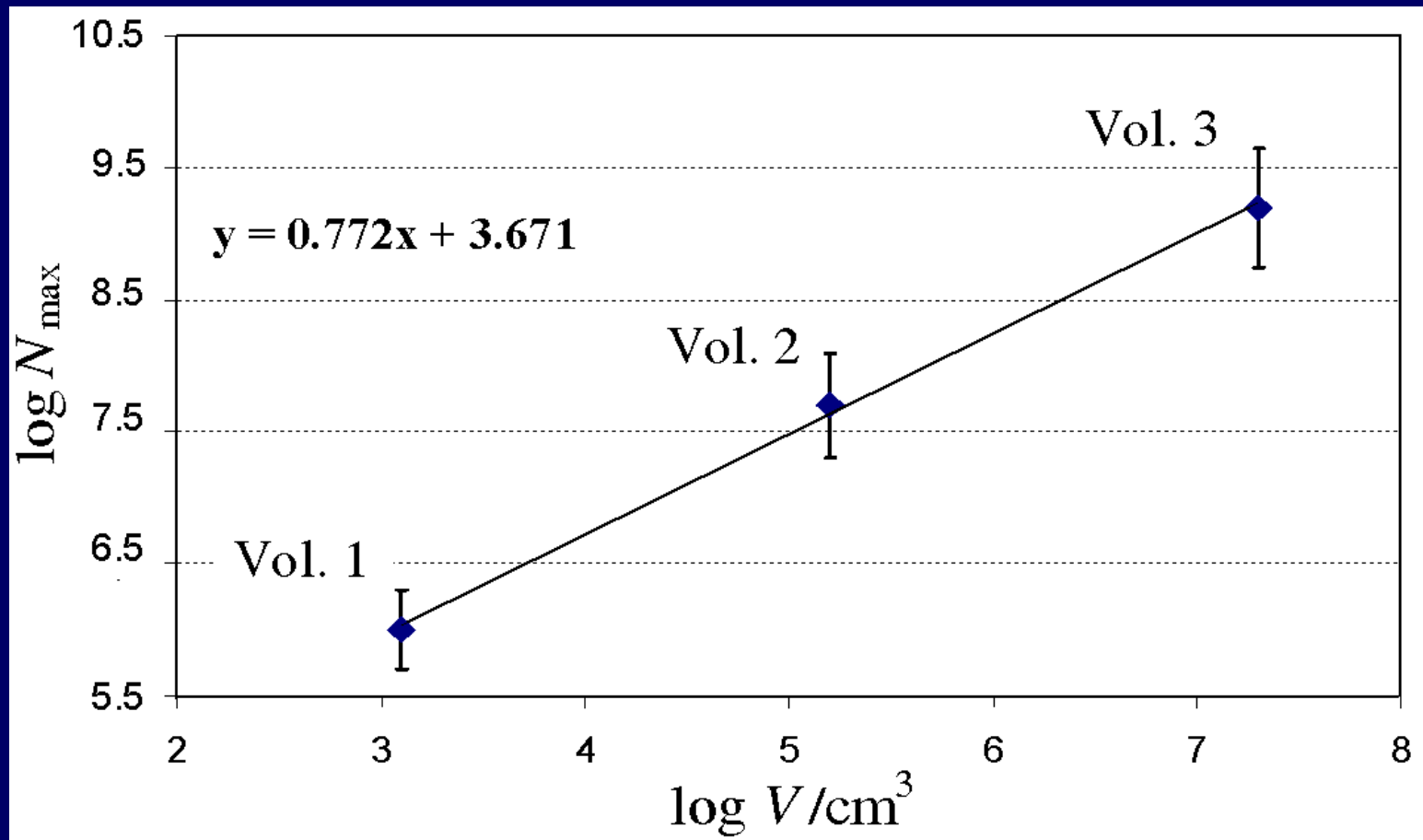
D: fractal exponent, comprised between 2 and 3.

(*) Carpinteri, A., Lacidogna, G., Pugno, N., “Structural Damage Diagnosis and Life-Time Assessment by Acoustic Emission Monitoring”. *Engineering Fracture Mechanics*, 74, 273-289 (2007).

Geometries of the tested specimens



Determination of the fractal dimension D



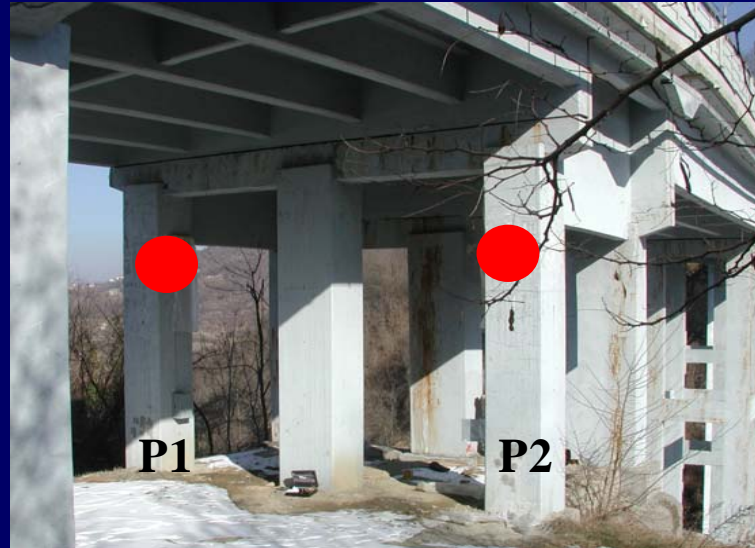
$$D \cong 2.31$$

AE long-term monitoring



Highway viaduct built in the 1950s

The viaduct and the monitored pilasters P₁ and P₂

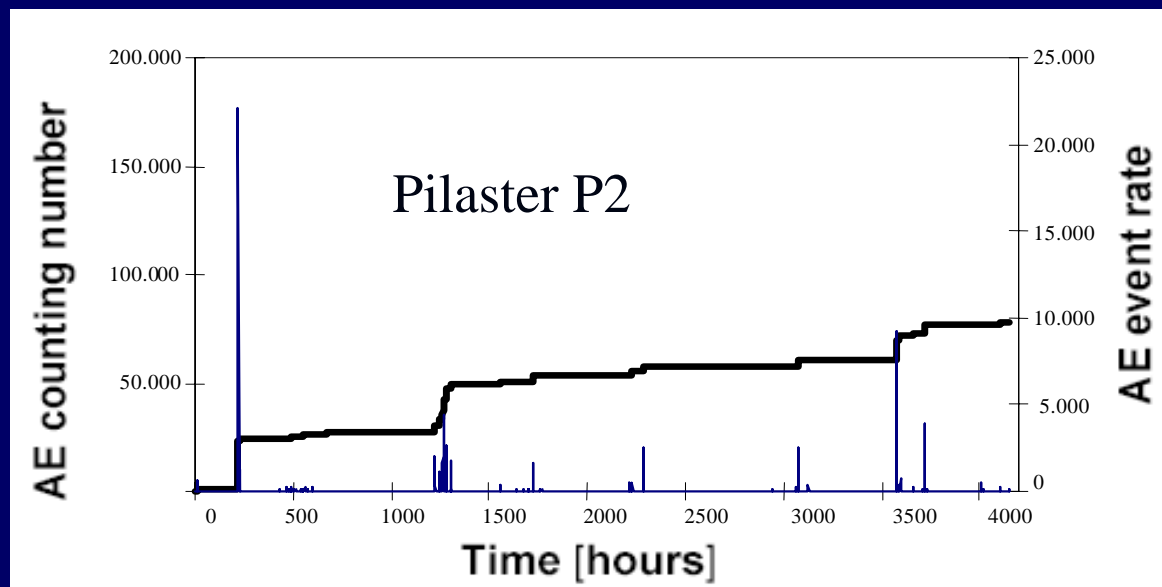
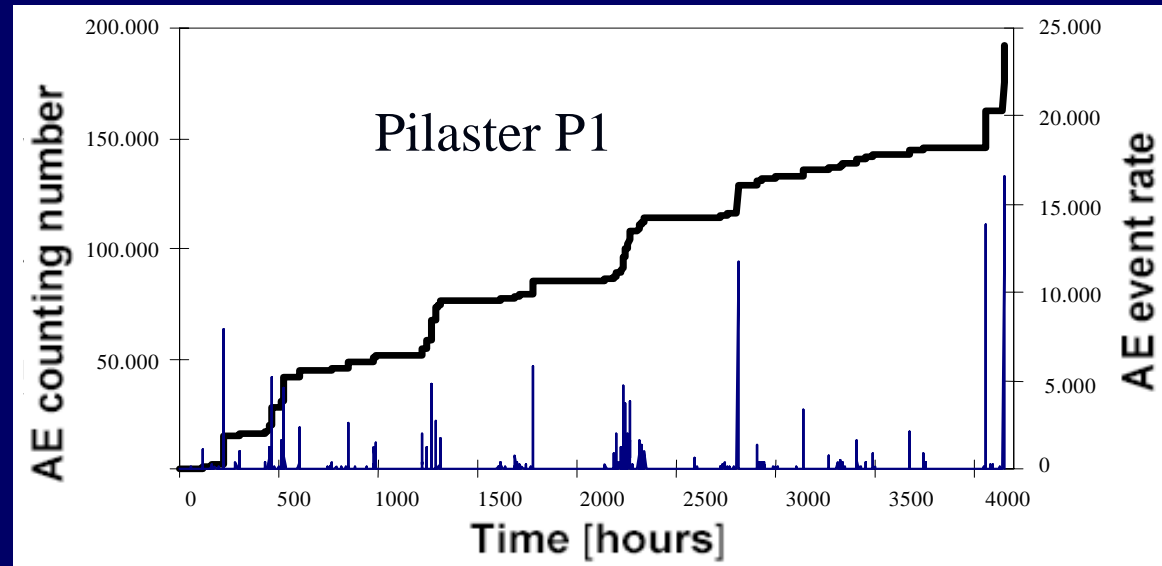


● AE sensors
location points

Cracks in pilaster P1 and the applied sensor



Pilasters P1 and P2 monitoring data



Assessment scheme

$$N_{\max} = N_{\max r} \left(\frac{V}{V_r} \right)^{D/3}$$

N_{\max} = critical number of AE events in the structure

$N_{\max r}$ = critical number of AE events in the reference specimen

V, V_r = volume of structure, reference specimen

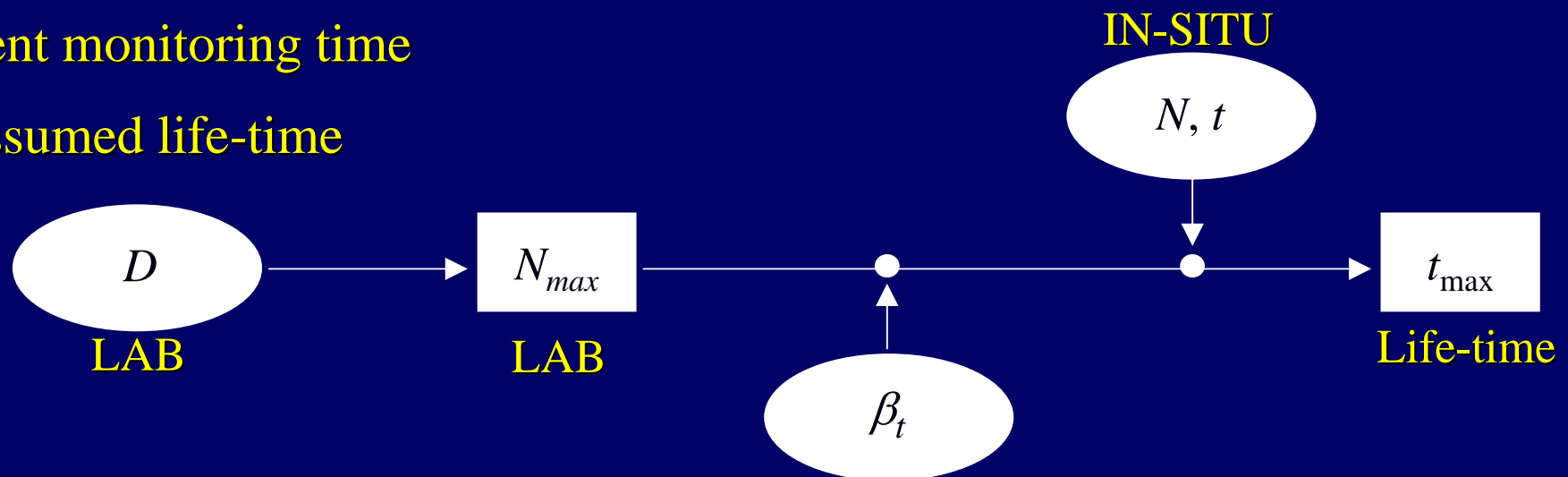
D = fractal exponent (from lab tests)

$$\frac{N}{N_{\max}} = \left(\frac{t}{t_{\max}} \right)^{\beta_t}$$

N = current cumulated number of AE events in the structure

t = current monitoring time

t_{\max} = assumed life-time



AE FREQUENCY-MAGNITUDE STATISTICS

Along the lines of earthquake seismology, the *magnitude* in terms of AE technique is defined as follows:

$$m = \text{Log}_{10} A_{\max} + f(r), \quad (2)$$

A_{\max} : signal amplitude, measured in microvolt;

$f(r)$: correction taking into account that the amplitude is a decreasing function of the distance r between the source and the sensor.

In seismology, earthquakes of larger magnitude occur less frequently than earthquakes of smaller magnitude. This fact can be quantified in terms of a magnitude-frequency relation, proposed by Gutenberg and Richter (1954) in an empirical way:

$$\text{Log}_{10}N(\geq m) = a - bm, \quad \text{or} \quad N(\geq m) = 10^{a-bm}, \quad (3)$$

N : cumulative number of earthquakes with magnitude $\geq m$, in a specified area and over a specified time span;

a, b : positive constants varying from region to region.

***b*-value analysis**

The aim is to establish a theoretical basis for considering the critical value $b = 1$, as observed both in AE laboratory tests and in tests performed on full sized engineering structures. By analogy with earthquakes, the AE damage size-scaling entails the validity of the relationship:

$$N(\geq L) = c L^{-D}, \quad (4)$$

N : cumulative number of AE events generated by source defects with a characteristic linear dimension $\geq L$;

L : linear dimension of the source defects;

c : constant of proportionality;

$D = 2b$: fractal dimension of the damaged domain.

The cumulative distribution (4) is substantially identical to the cumulative distribution proposed by Carpinteri (*), which gives the probability of a defect of size $\geq L$ being present in a body:

$$P(\geq L) \propto L^{-\gamma}, \quad (5)$$

Therefore, the number of defects with size $\geq L$ is:

$$N(\geq L) = N_{tot} L^{-\gamma}, \quad (6)$$

N_{tot} : total number of defects in the body;

γ : exponent measuring the degree of disorder, i.e. the scatter in the defect size distribution.

(*) Carpinteri, A., "Scaling laws and Renormalization Groups for Strength and Toughness of Disordered Materials". *International Journal of Solids and Structures*, 31, 291-302 (1994).

By equating distributions (4) and (6) it is found that:

$$2b = \gamma. \quad (7)$$

As shown by Carpinteri (*Int. J. of Solids and Structures*, 31, 291-302 (1994))

$$\gamma = 2$$

is the exponent of the *defect size distribution of self-similarity* in a body, where the maximum defect size is proportional to the characteristic size of the body.

It was found that this exponent corresponds to the maximum disorder in the defect size distribution. From Eq. (7) we obtain the *critical value*

$$b = 1$$

which is experimentally approached in structural members during the final crack propagation.



Loading test with AE sources localization

Scheme of the beam cross-section

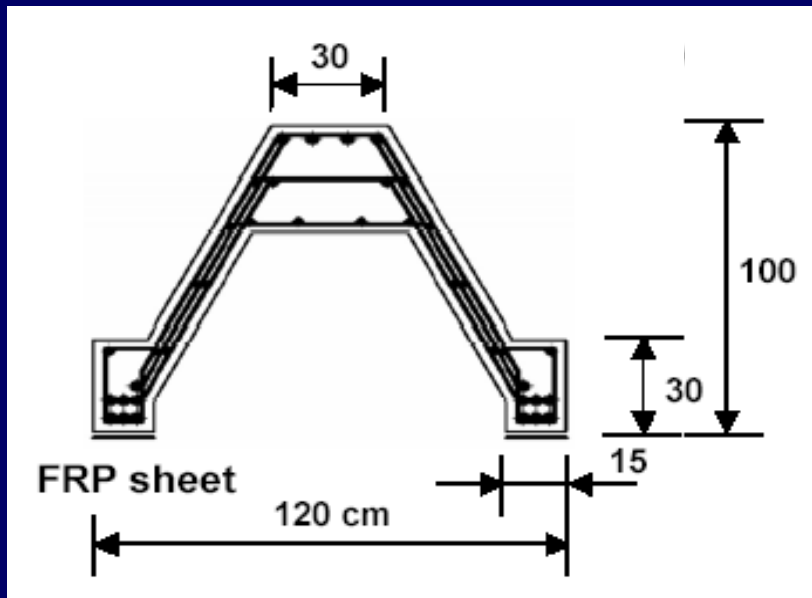
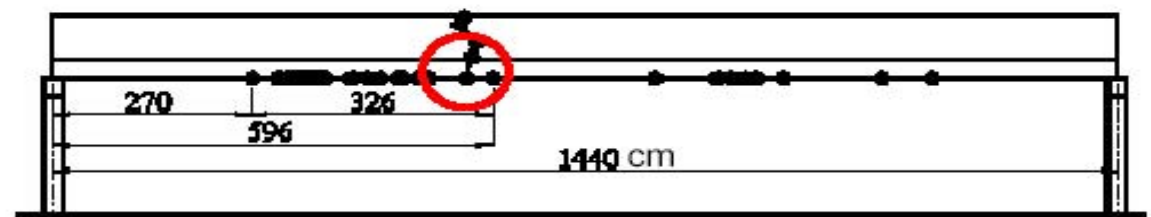
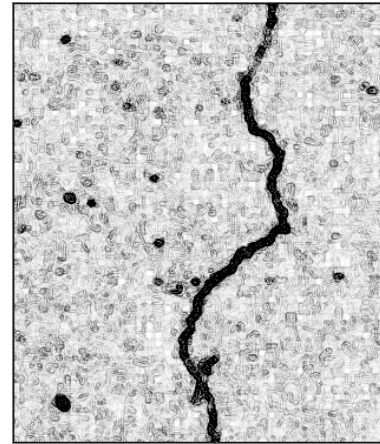
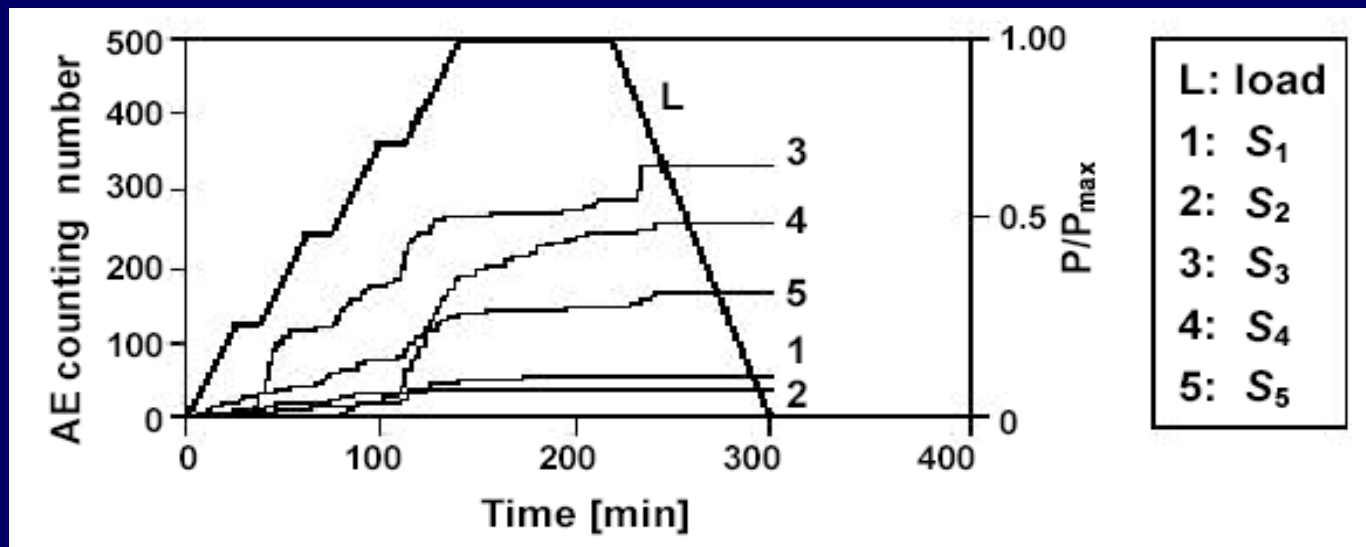


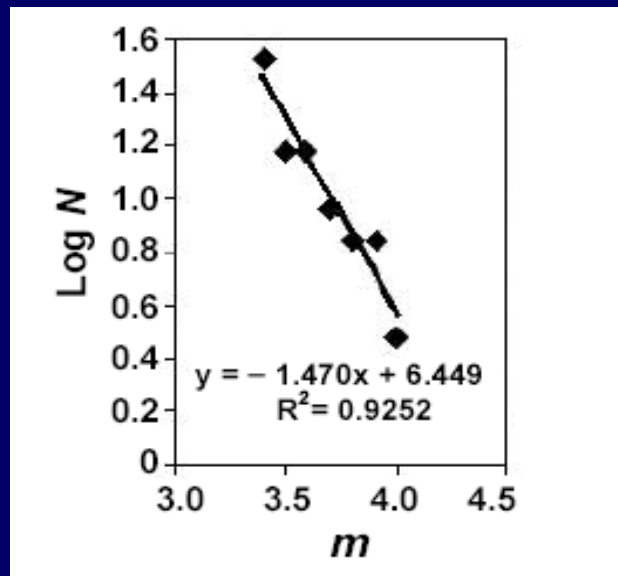
Photo of a localized crack



Scheme of the beam indicating localized AE sources

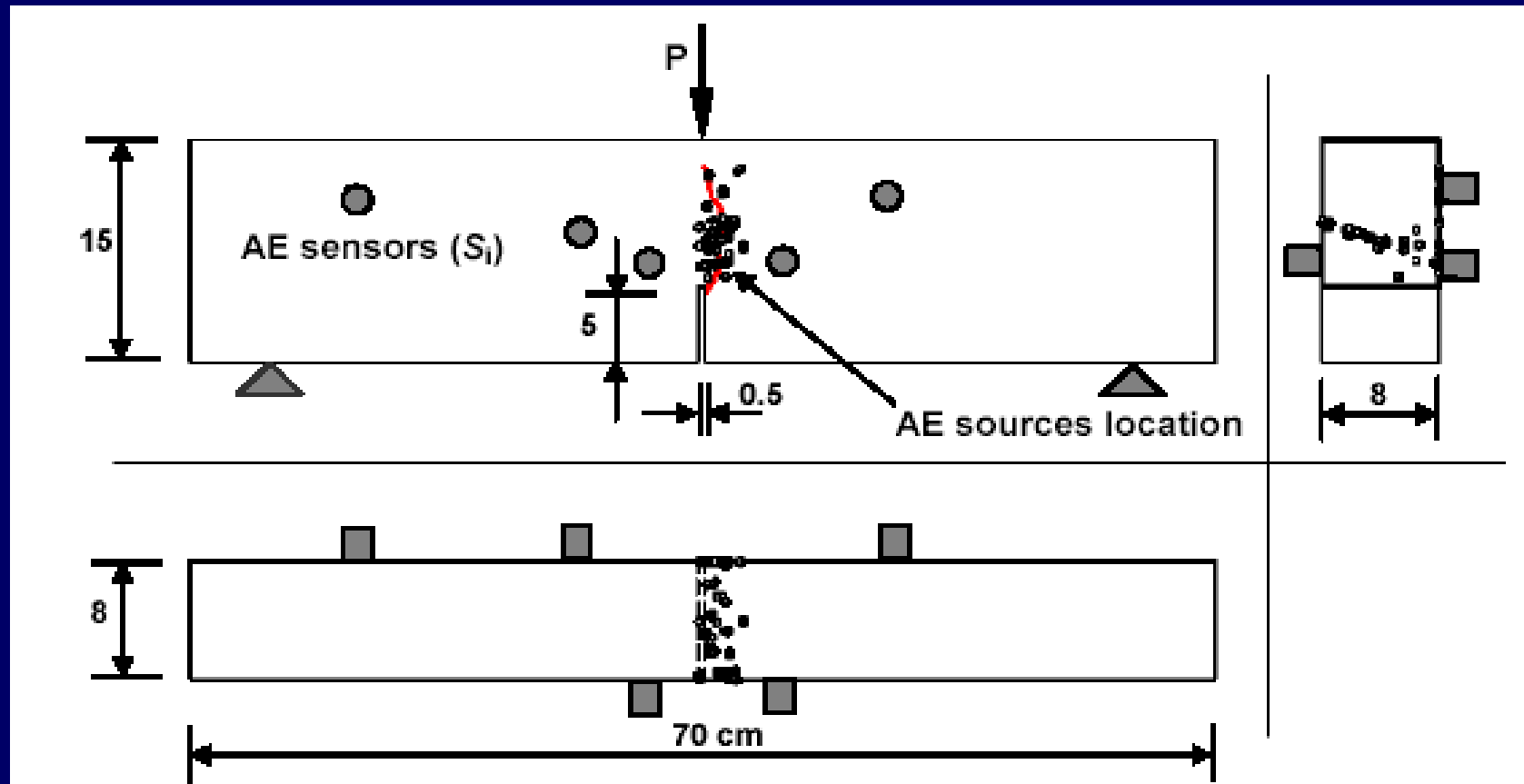


AE counting number for each sensor S_i during the loading test

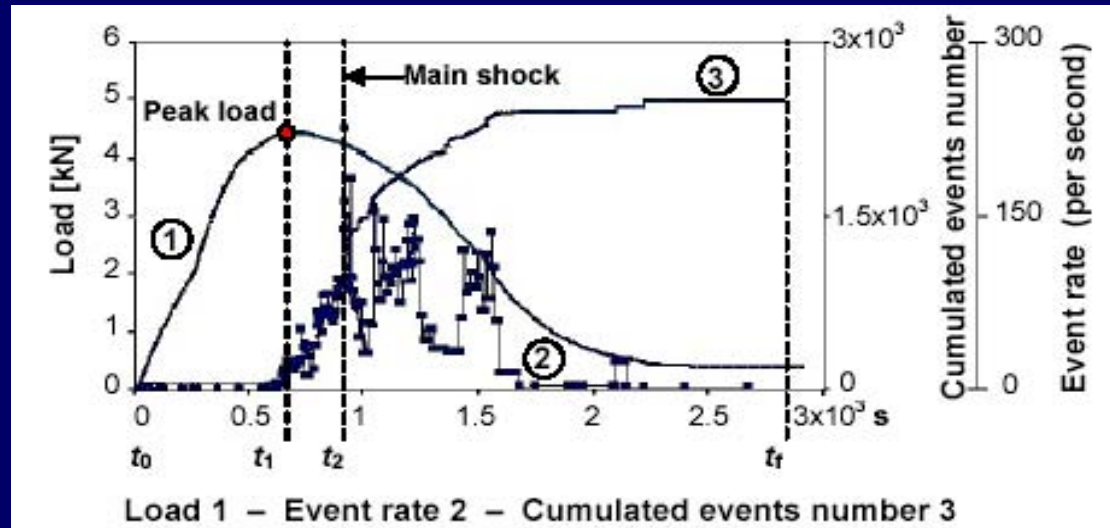


b -value during the loading test

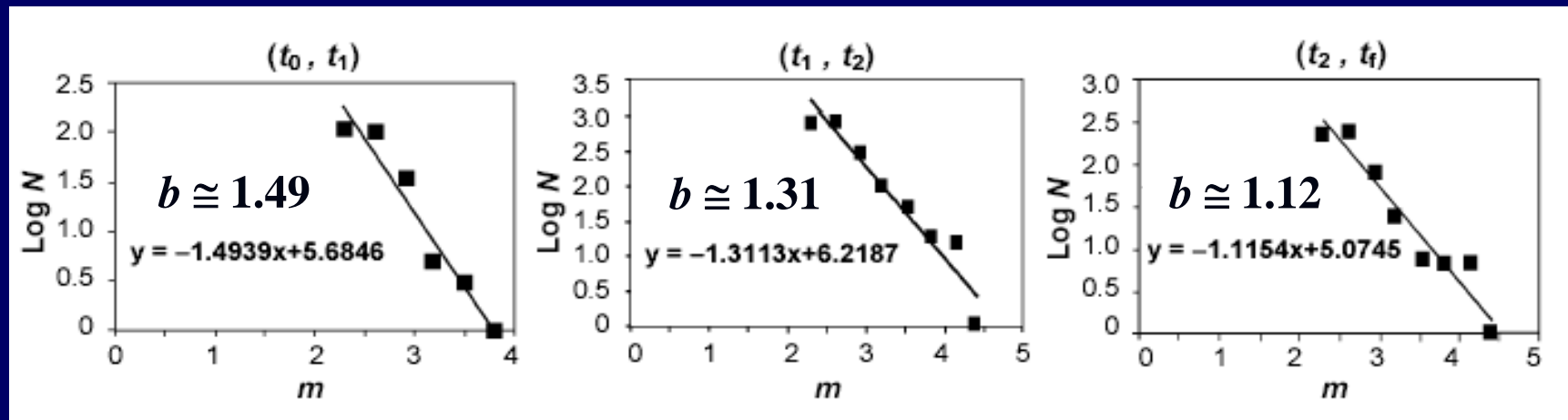
Three-Point Bending Test



Identification of the fracture process zone

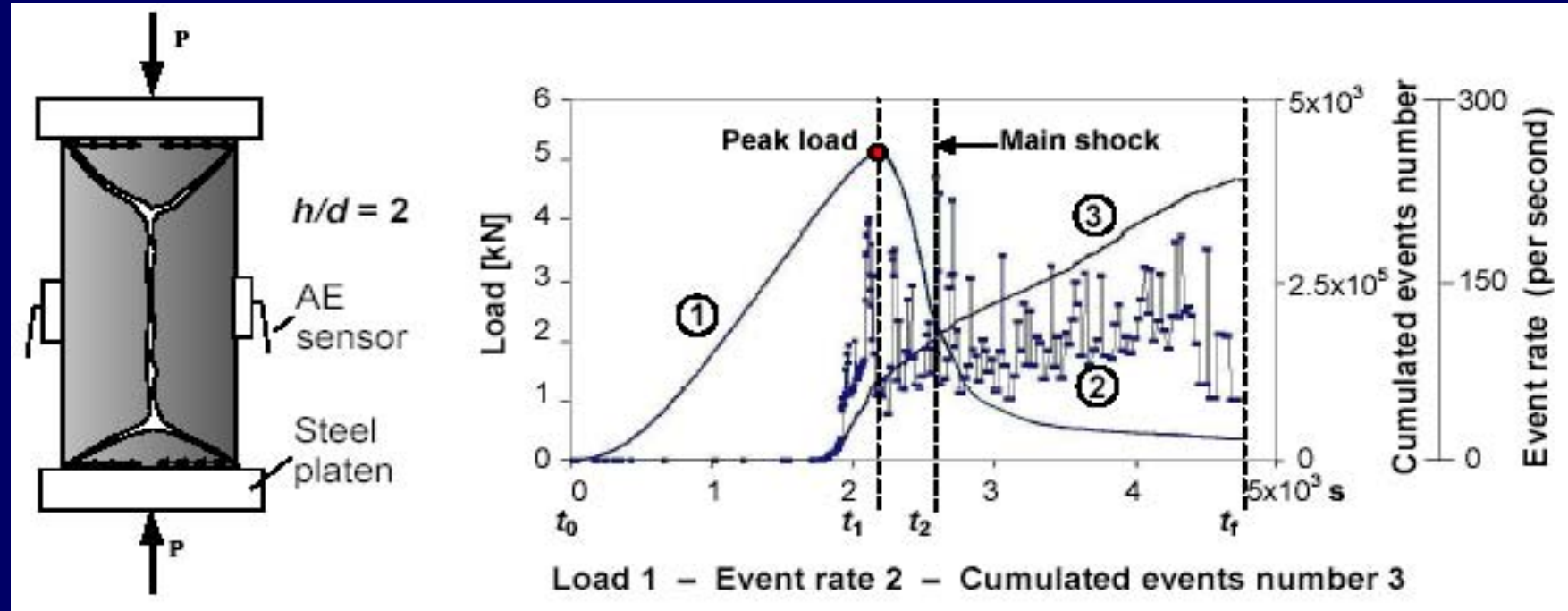


Load vs. time curve and AE activity

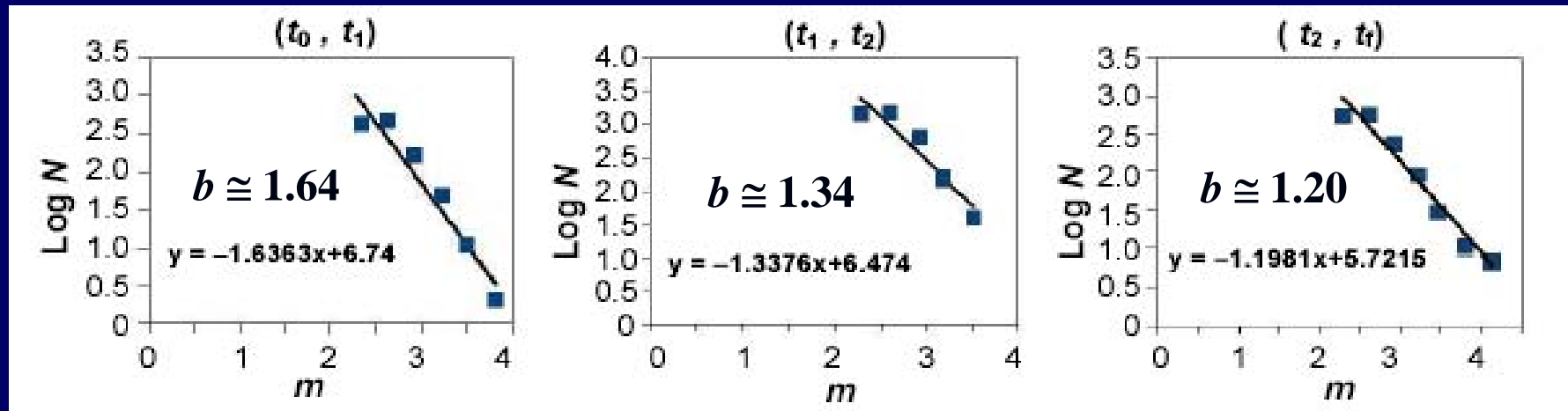


b-values during the loading test

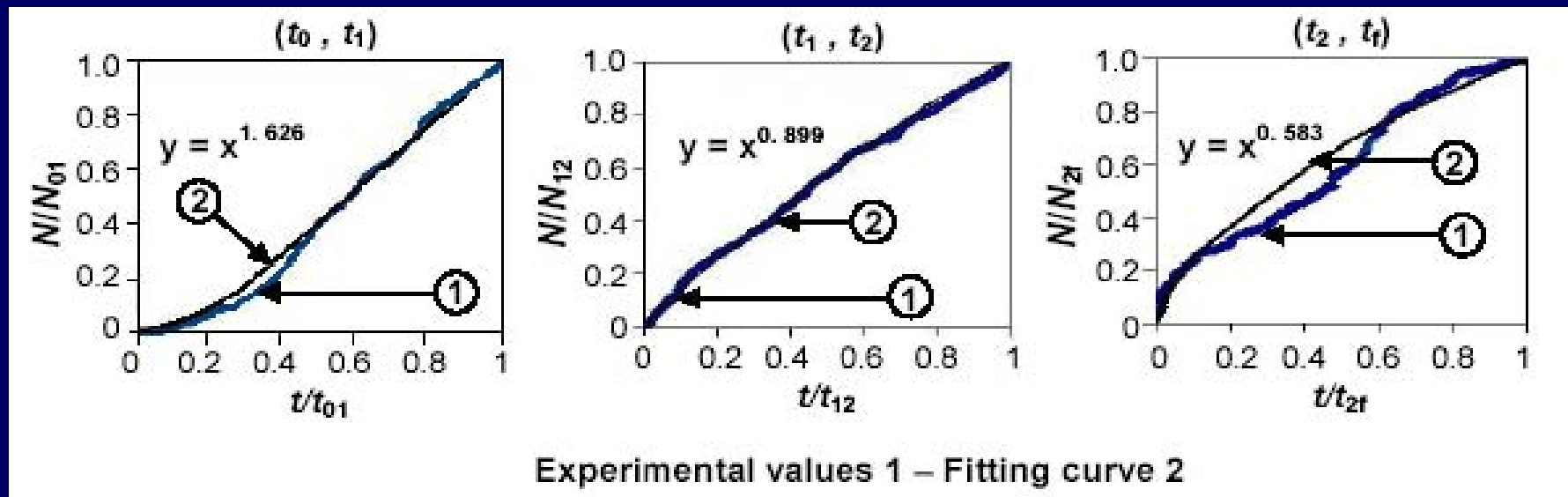
Concrete Specimen in Compression



Load vs. time curve and AE activity



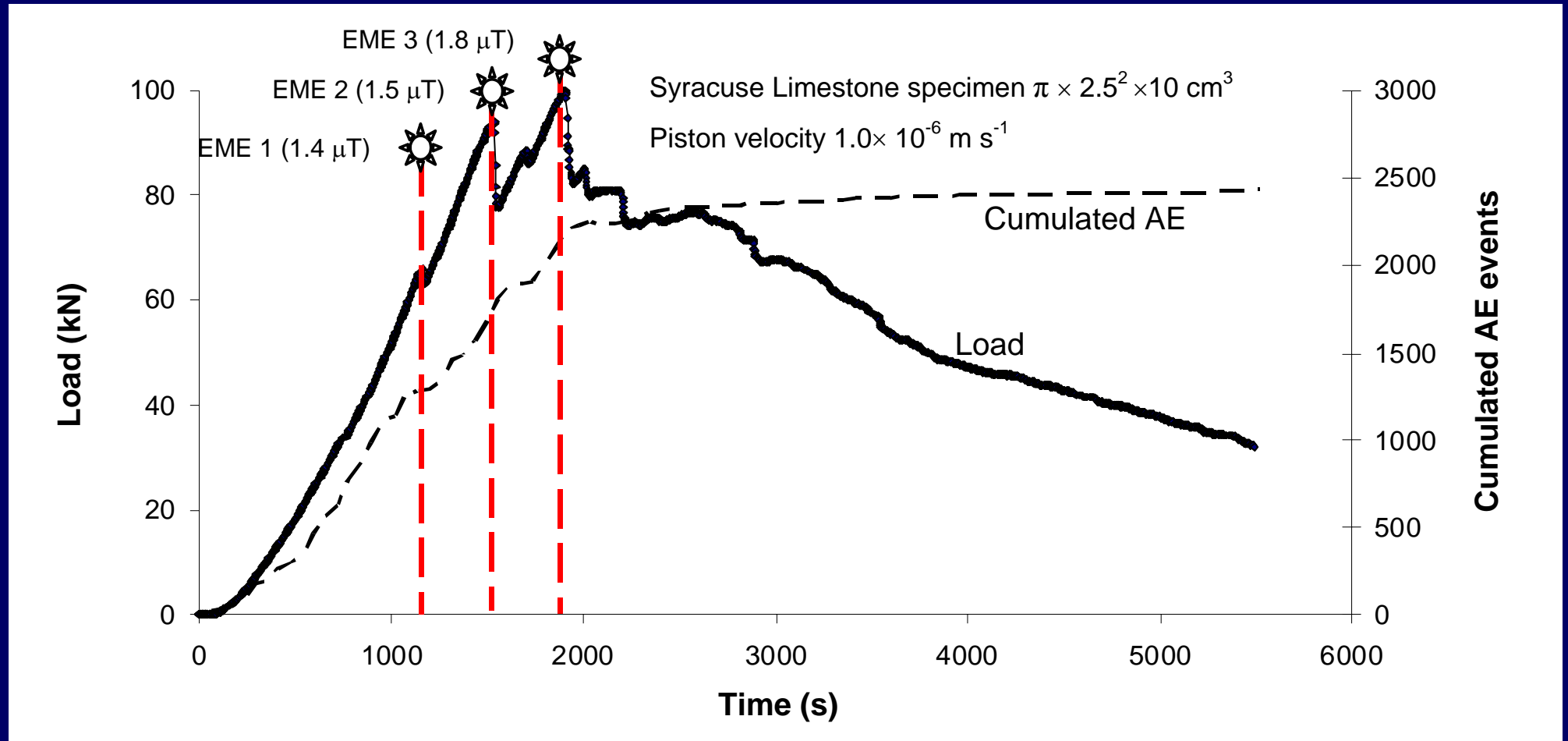
b -values during the loading test



Variation in β_t parameter during the loading test

ELECTROMAGNETIC EMISSIONS

Syracuse Limestone Specimen



The dashed line represents the cumulated number of AE

The stars on the graph show the moments of EME events with magnetic component comprised between 1.4 and 1.8 μT

PIEZONUCLEAR REACTIONS IN COMPRESSED SOLIDS

Neutron emission measurements by means of helium-3 neutron detectors were performed on solid test specimens during crushing failure.

The materials used were marble and granite, selected in that they present a different behaviour in compression failure (i.e., a different brittleness index) and a different iron content. All the test specimens were of the same size and shape.

Neutron emissions from the granite test specimens were found to be about one order of magnitude larger than the natural background level at the time of failure.

These neutron emissions were caused by piezonuclear reactions that occurred in the granite, but did not occur in the marble.

(*) Carpinteri, A., Cardone, F., Lacidogna, G., “Piezonuclear neutrons from brittle fracture: Early results of mechanical compression tests”, *Strain*, 45, 332-339 (2009).

(**) Cardone, F., Carpinteri, A., Lacidogna, G., “Piezonuclear neutrons from fracturing of inert solids”, *Physics Letters A*, 373, 4158-4163 (2009).

Experimental set-up

During the experimental analysis four test specimens were used:

- two made of Carrara marble, calcite, specimens P1 and P2;
- two made of Luserna granite, gneiss, specimens P3 and P4;
- all of them measuring $6 \times 6 \times 10 \text{ cm}^3$.

This choice was prompted by the consideration that, test specimen dimensions being the same, different brittleness coefficients would cause catastrophic failure in granite, not in marble.





Testing machine

The same testing machine was used on all the test specimens: a standard servo-hydraulic press Baldwin with a maximum capacity of 500 kN, equipped with control electronics.

The tests were performed in piston travel displacement control by setting, for all the test specimens, a velocity of 10^{-6} m/s during compression.

Neutron emission measurements were made by means of a helium-3 detector placed at a distance of 10 cm from the test specimen.

The detector was enclosed in a polystyrene case to prevent the results from being altered by by impacts and vibrations.





Two views of neutron detection by thermodynamic detectors
type BD (bubble detector/dosimeter)
manufactured by Bubble Technology Industries (BTI)

Neutron emission measurements

Before the loading tests

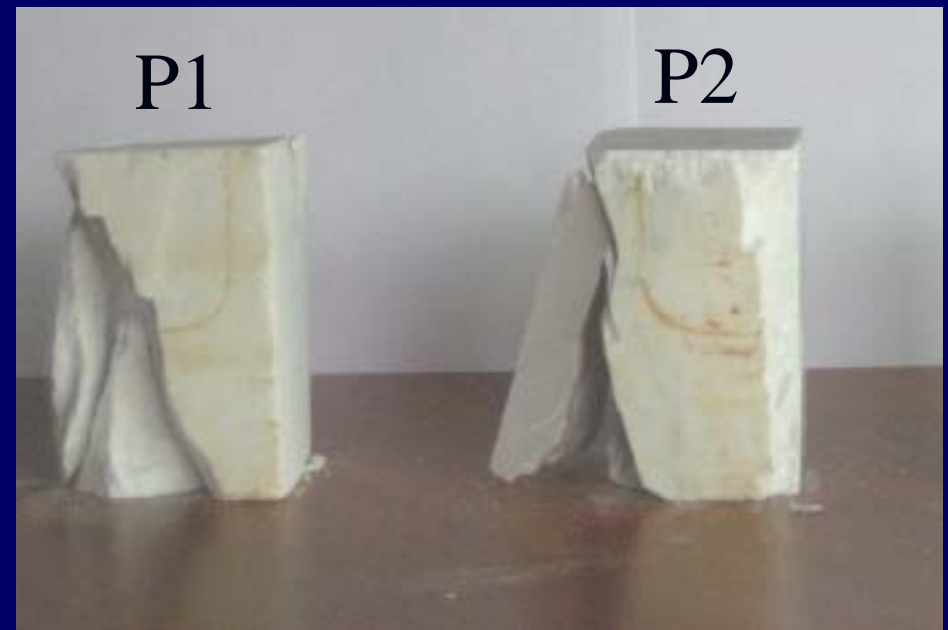
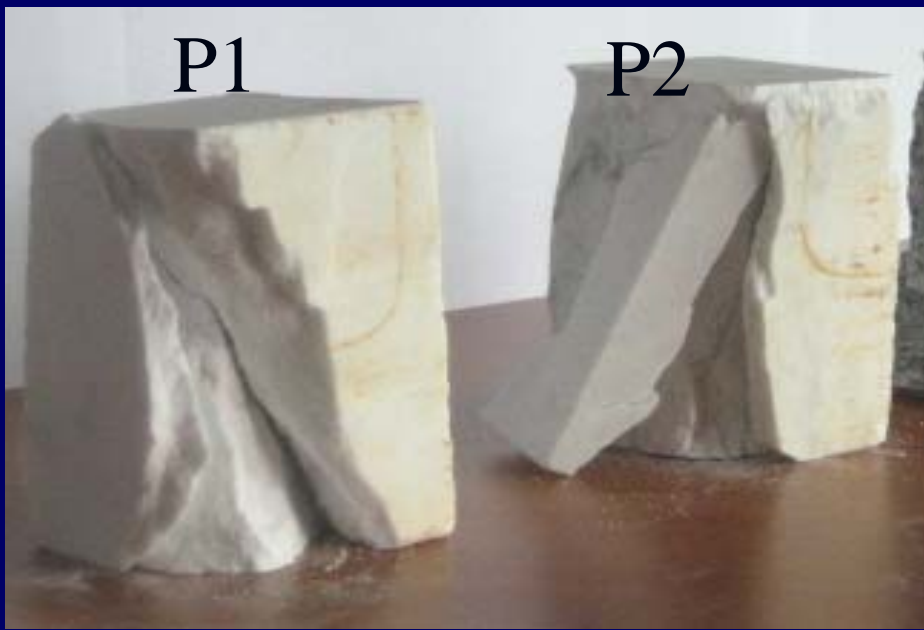
The neutron background was measured at 600 s time intervals to obtain sufficient statistical data with the detector in the position shown in the previous figure.

The average background count rate was:

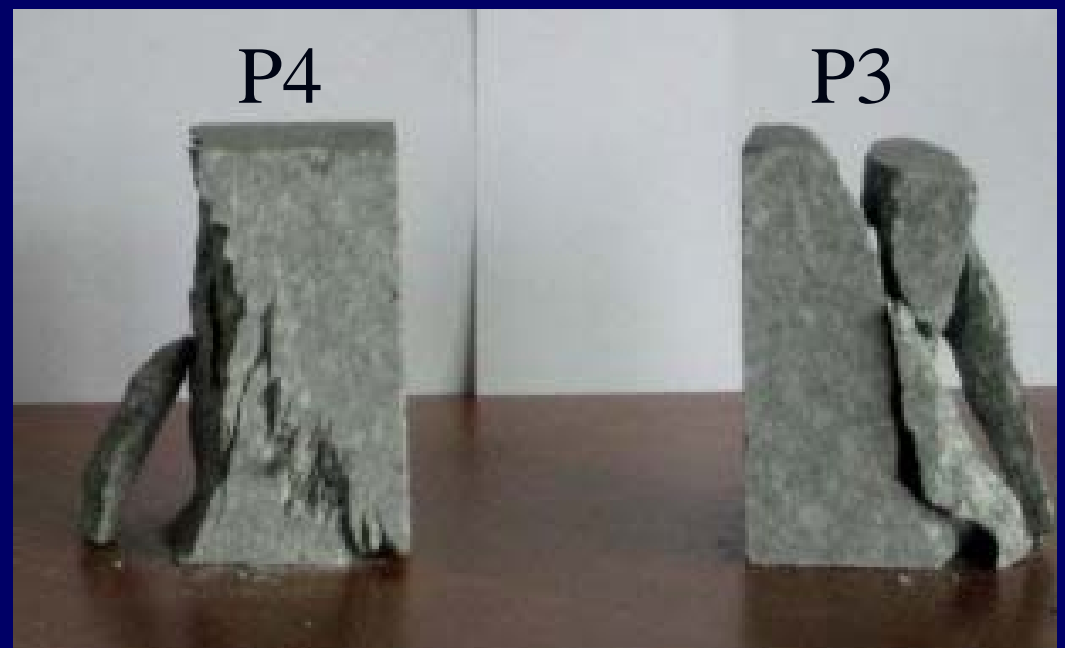
$$3.8 \times 10^{-2} \pm 0.2 \times 10^{-2} \text{ cps.}$$

During the loading tests

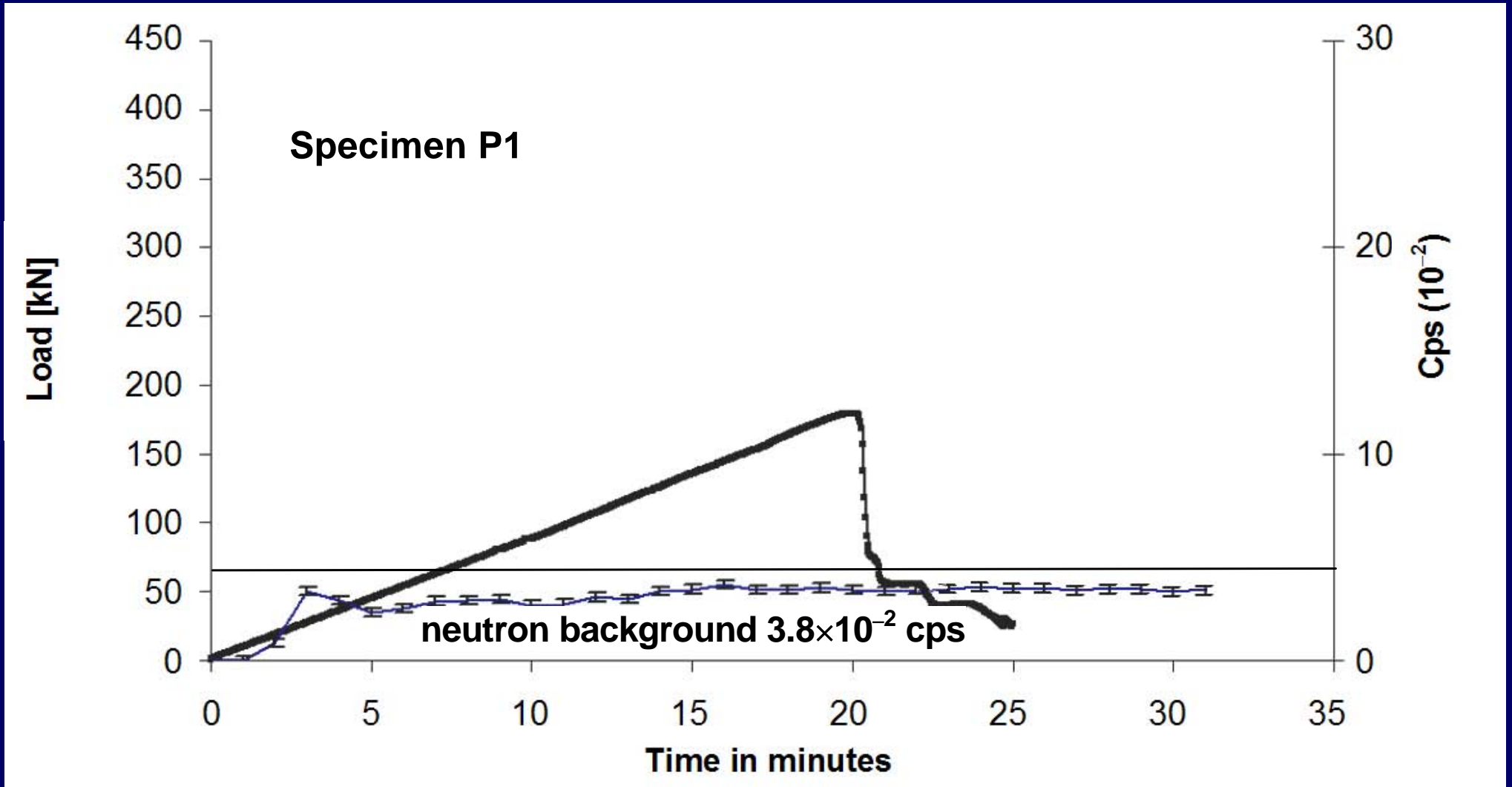
- The neutron measurements obtained on the two Carrara marble specimens yielded values comparable with the background, even at the time of test specimen failure.
- The neutron measurements obtained on the two Luserna granite specimens, instead, exceeded the background value by about one order of magnitude at the test specimen failure.



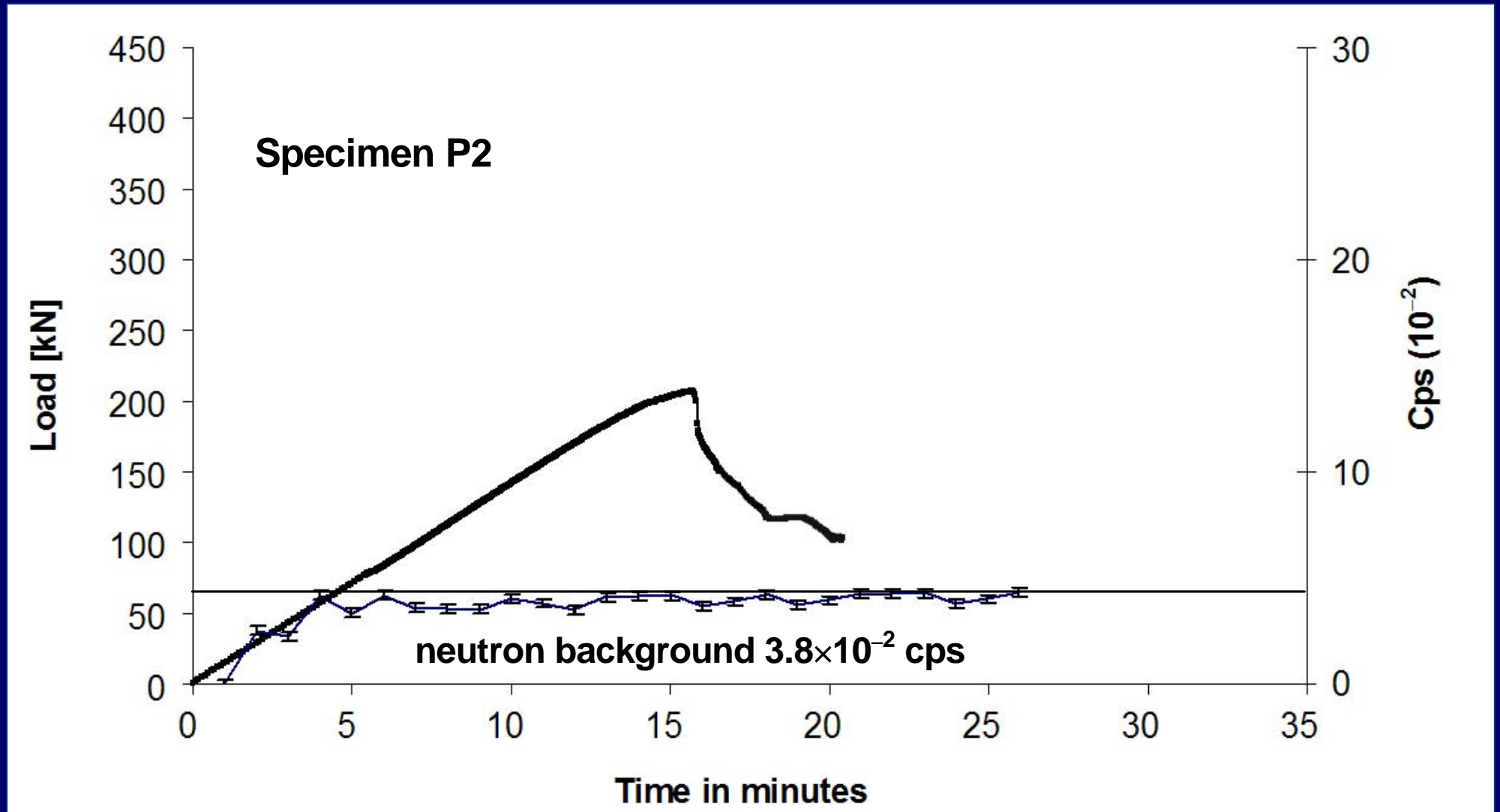
Specimens P1 and P2 in Carrara marble following compression failure.



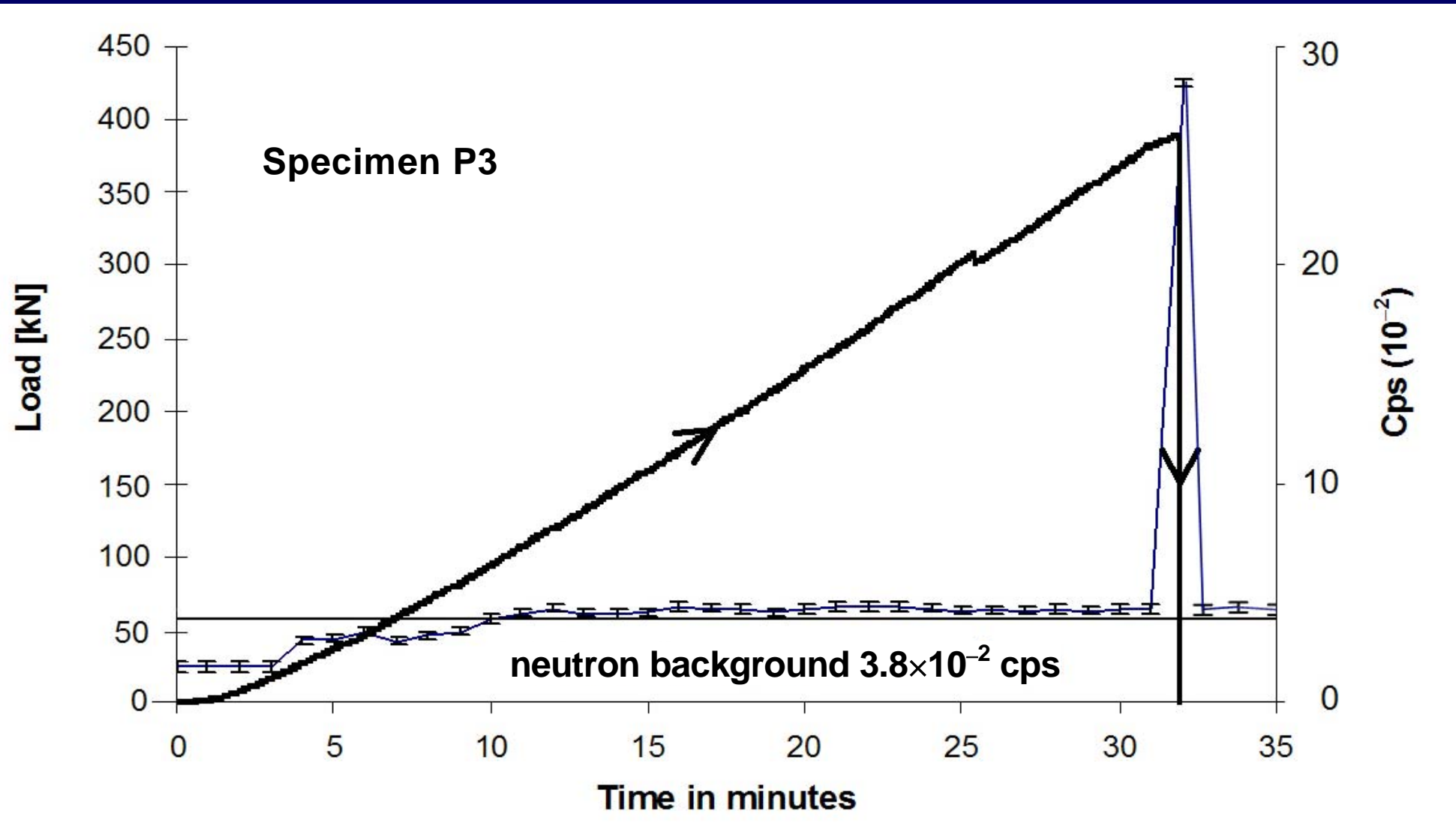
Specimens P3 e P4 in Luserna granite following compression failure.



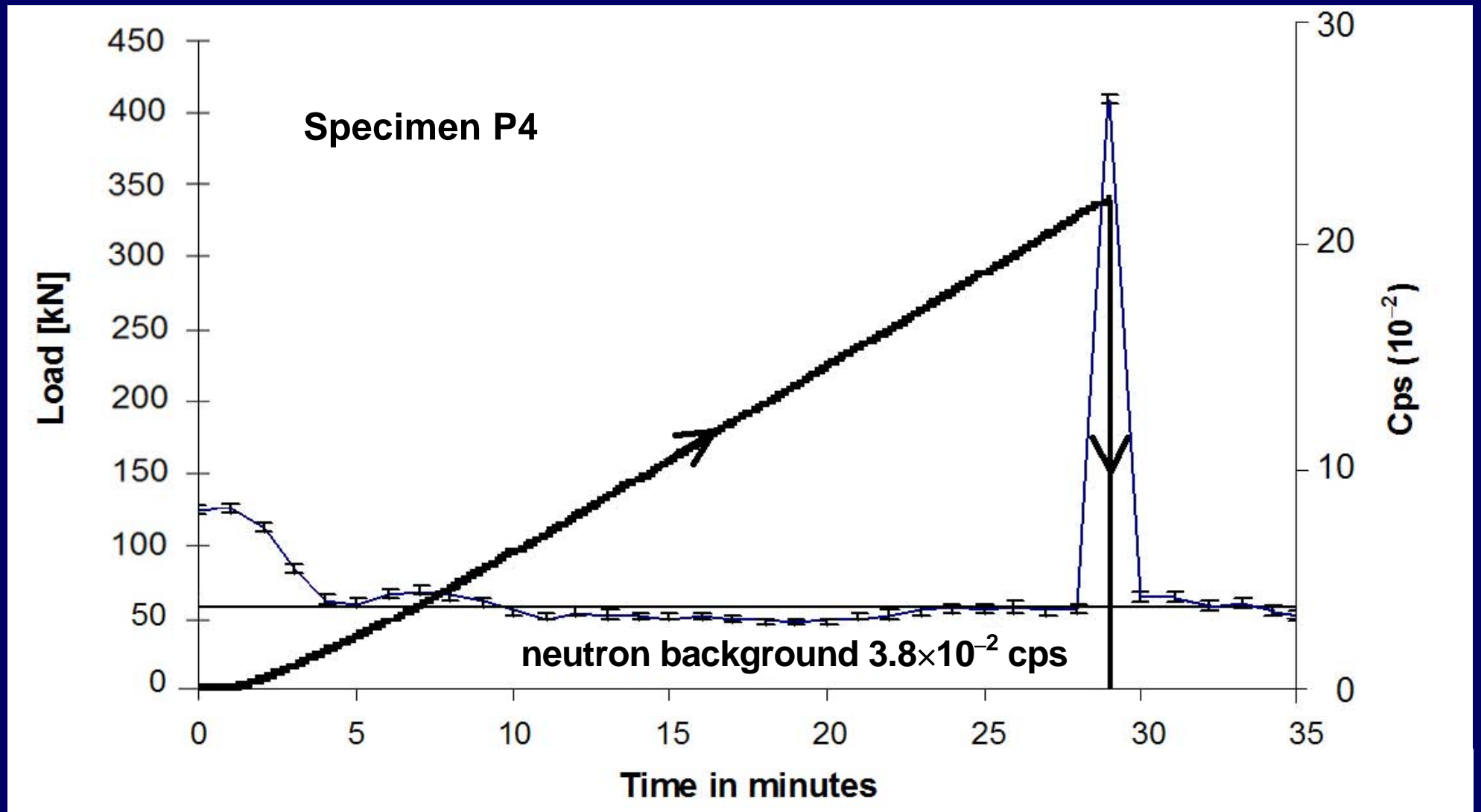
Load vs. time and cps curve for P1 test specimen in Carrara marble.



Load vs. time and cps curve for P2 test specimen in Carrara marble.

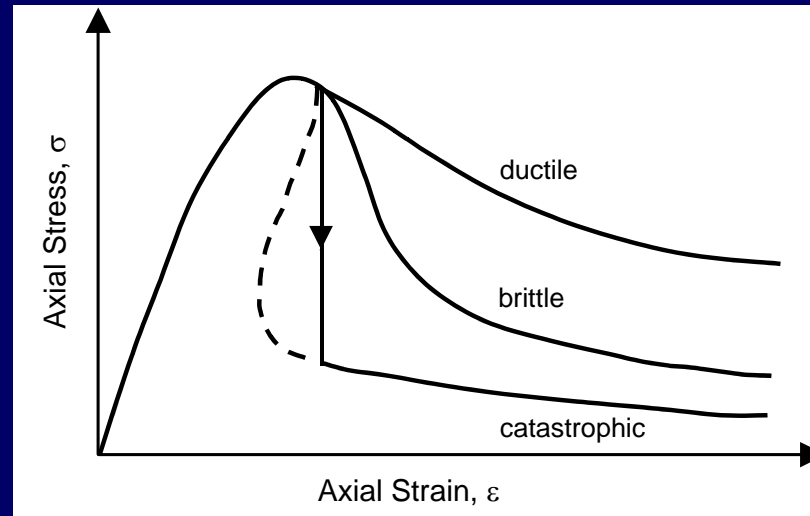


Load vs. time and cps curve for P3 test specimen in Luserna granite.

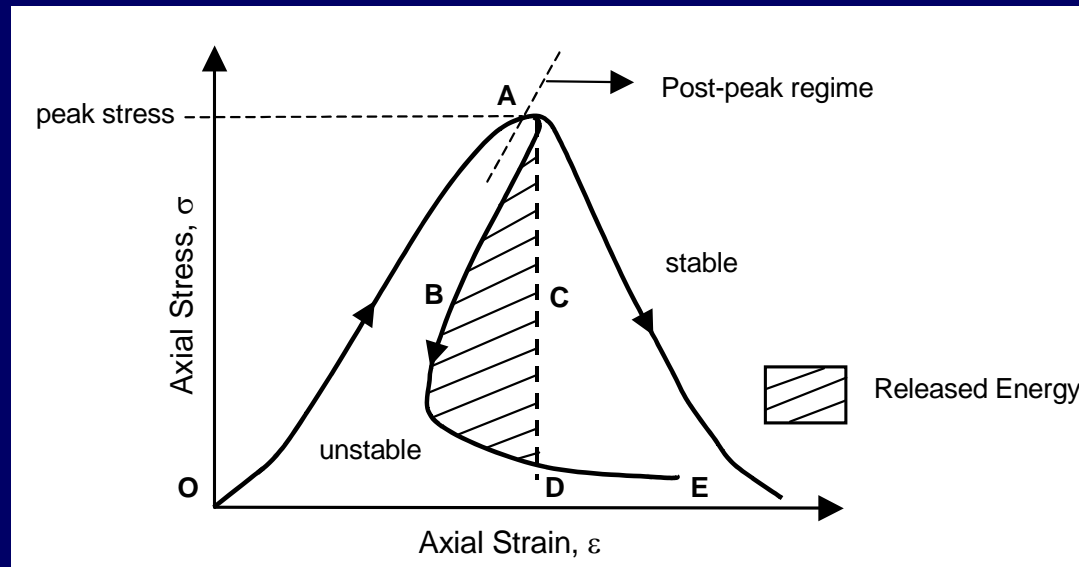


Load vs. time and cps curve for P4 test specimen in Luserna granite.

Ductile, brittle and catastrophic behaviour

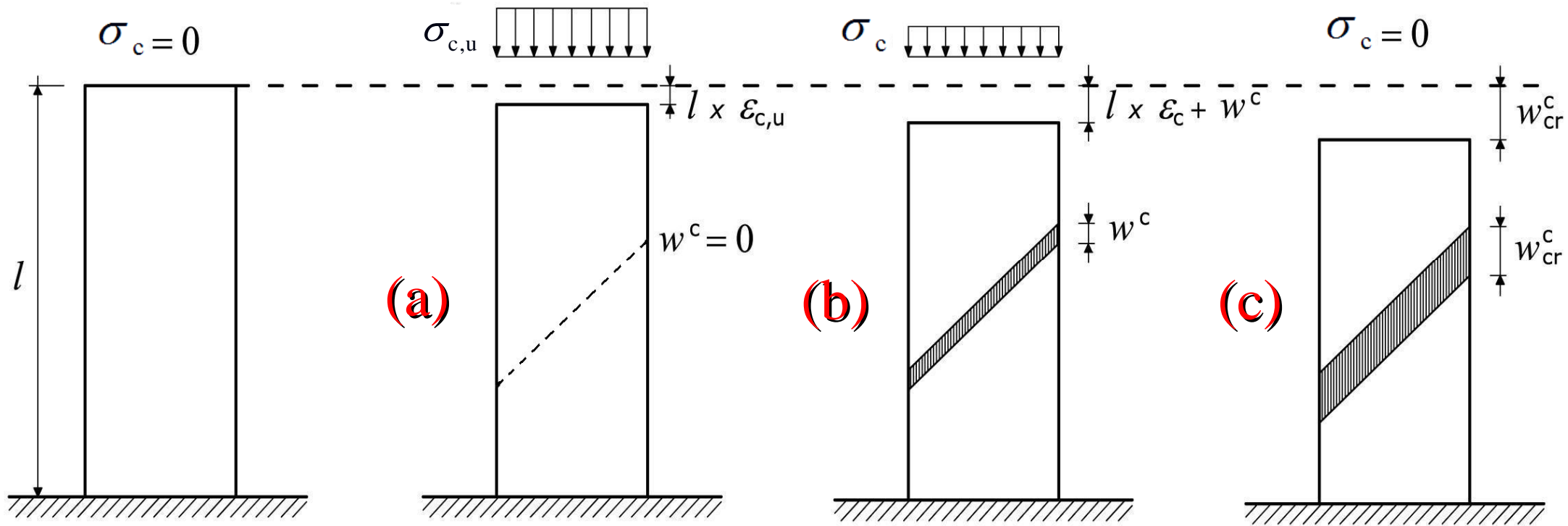


Ductile, brittle and catastrophic behaviour



Energy release and stable vs. unstable stress-strain behaviour

Subsequent stages in the deformation history of a specimen in compression^(*) ^(**)



$$\delta = \epsilon_c l = \frac{\sigma_c}{E} l;$$

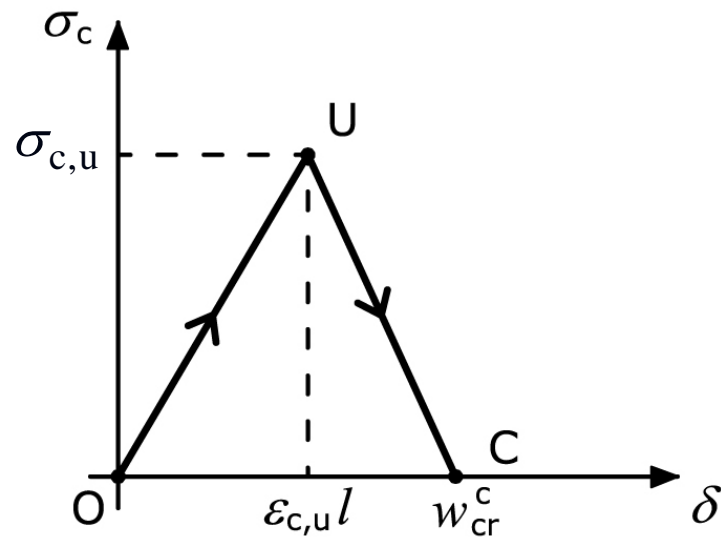
$$\delta = \frac{\sigma_c}{E} l + w^c;$$

$$\delta \geq w_{cr}^c.$$

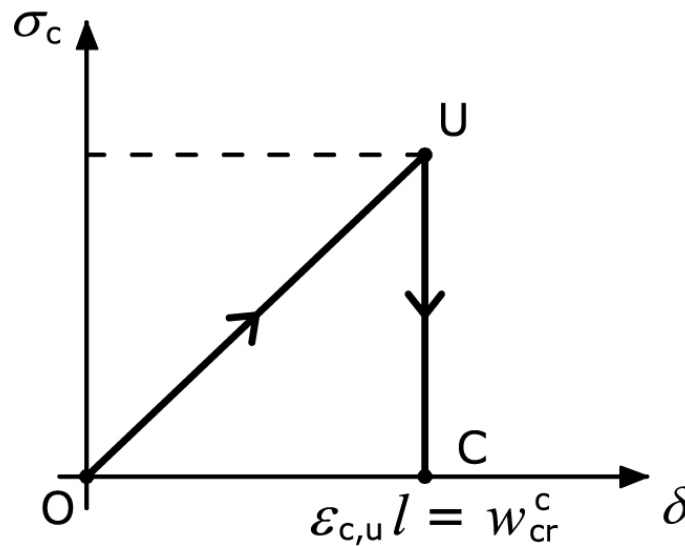
(*) Carpinteri, A., "Cusp catastrophe interpretation of fracture instability", *J. of Mechanics and Physics of Solids*, 37 (5), 567–582 (1989).

(**) Carpinteri, A., Corrado, M., "An extended (fractal) overlapping crack model to describe crushing size-scale effects in compression", *Eng. Failure Analysis*, in print.

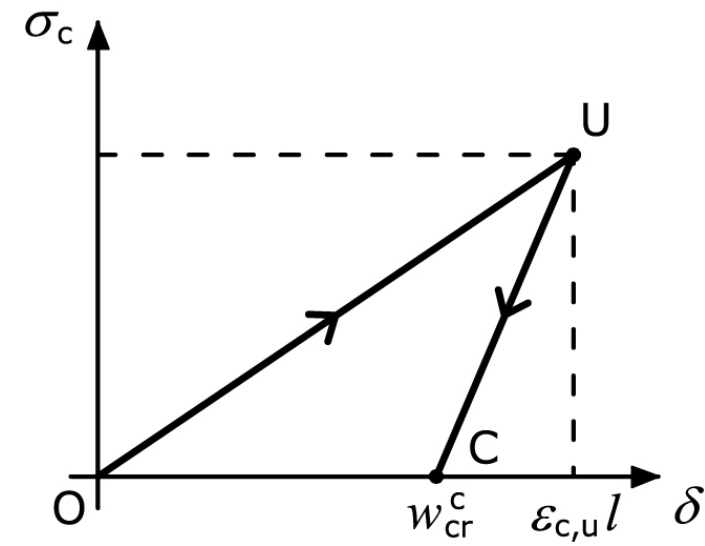
Stress vs. displacement response of a specimen in compression



**Normal
softening**



**Vertical
drop**



**Catastrophic
behaviour**

Elastic strain energy at the peak load, ΔE

Test specimen	Material	ΔE [J]
P1	Carrara marble	124
P2	Carrara marble	128
P3	Luserna granite	384
P4	Luserna granite	296

Threshold of energy rate for piezonuclear reactions (*)(**):

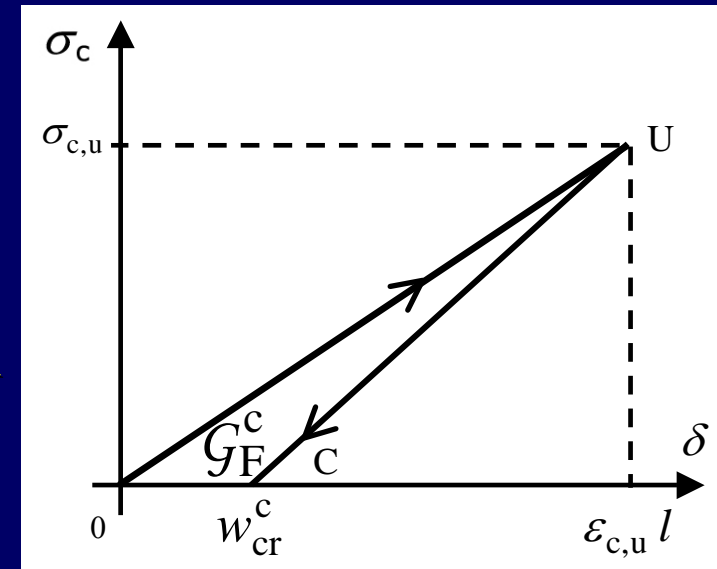
$$\frac{\Delta E}{\Delta t} \sim 7.69 \times 10^{11} \text{ W} \rightarrow \Delta t \sim 0.5 \text{ ns}$$

Extension of the energy release zone:

$$\Delta x = v \Delta t \sim 4000 \text{ m/s} \times 0.5 \text{ ns} \sim 2 \mu\text{m}$$

Comparison with the critical value of the interpenetration length:

$$\Delta x \sim w_{\text{cr}}^c ?$$



(*) Cardone, F., Mignani, R., “Piezonuclear reactions and Lorenz invariance breakdown”, *Int. J. of Modern Physics E, Nuclear Physics*, 15 (901), 911–924 (2006).

(**) Cardone, F., Mignani, R., *Deformed Spacetime*, Springer, Dordrecht, 2007, chaps 16 –17.

PIEZONUCLEAR REACTIONS IN CONCRETE SPECIMENS

Further neutron emission measurements by means of helium-3 neutron detector were performed on concrete specimens during crushing failure.

The materials used were normal concrete, and concrete with 10% of iron content addition. The test specimens were of different size and shape, with a slenderness from 0.5 to 4.

Neutron emissions were found to be three–four times larger than the natural background level in the case of catastrophic failure. Instead, in the specimens with more ductile behaviour, neutron emissions were found to be comparable with the ordinary background.

The neutron background was measured before the loading tests with the detector in the same position of experimental measurements.

The average measured background level was ranging from:

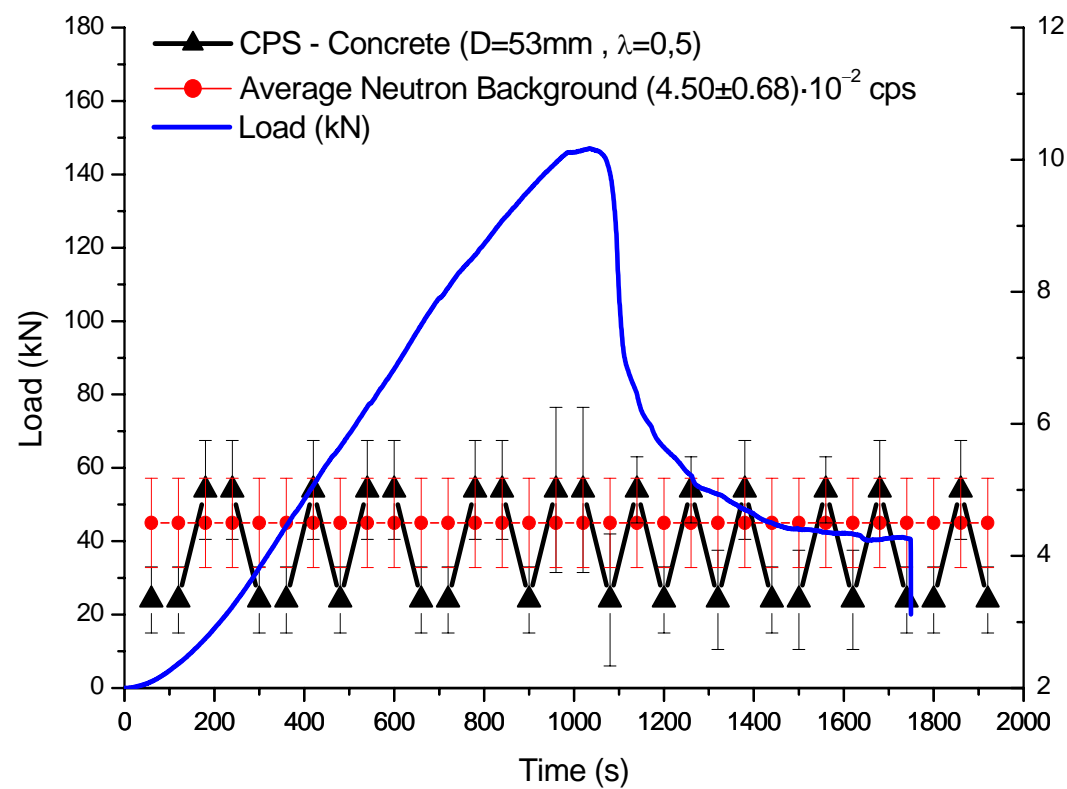
$$(3.61 \pm 0.54) \cdot 10^{-2} \text{ cps} \quad \text{to} \quad (4.80 \pm 0.72) \cdot 10^{-2} \text{ cps}$$

Experimental set-up

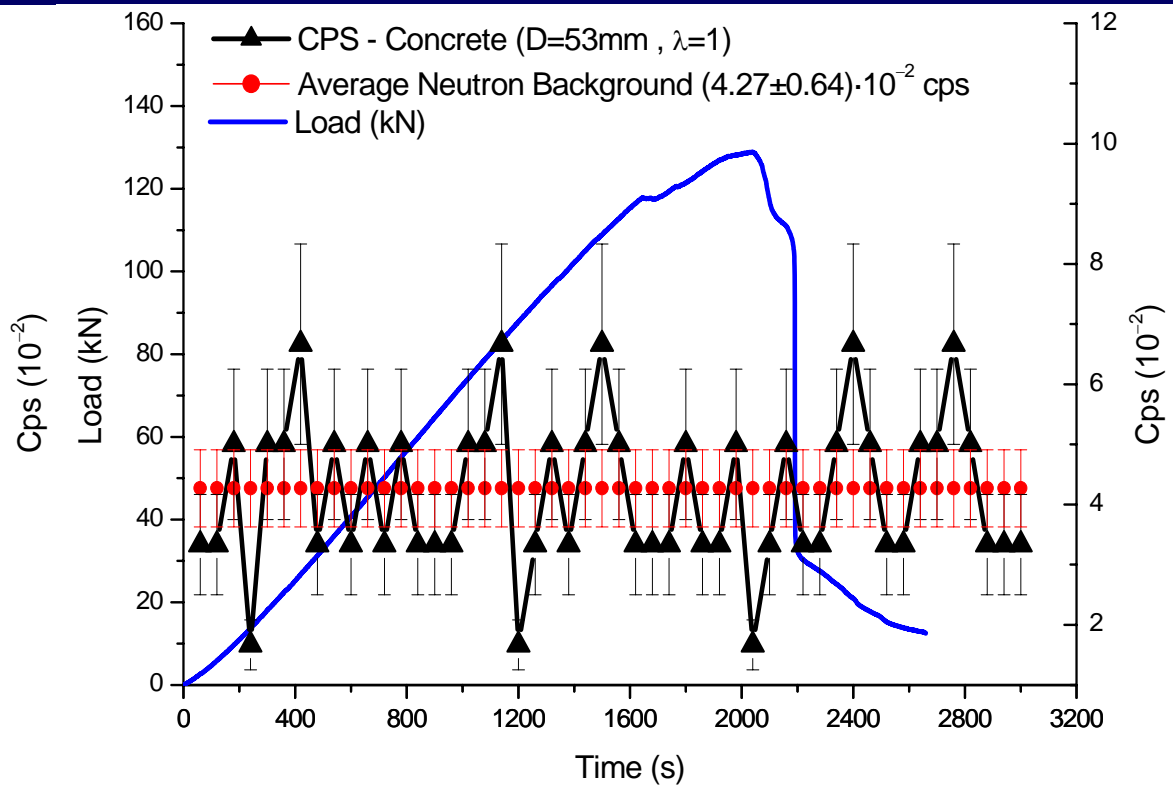
During the experimental analysis five test specimens were used:

- Normal concrete (C1, C2, C3, C4)
D = 53 mm, $\lambda = 0.5, 1, 2, 3$;
- Concrete with 10% iron content addition (C5)
40 × 40 × 160 mm³.

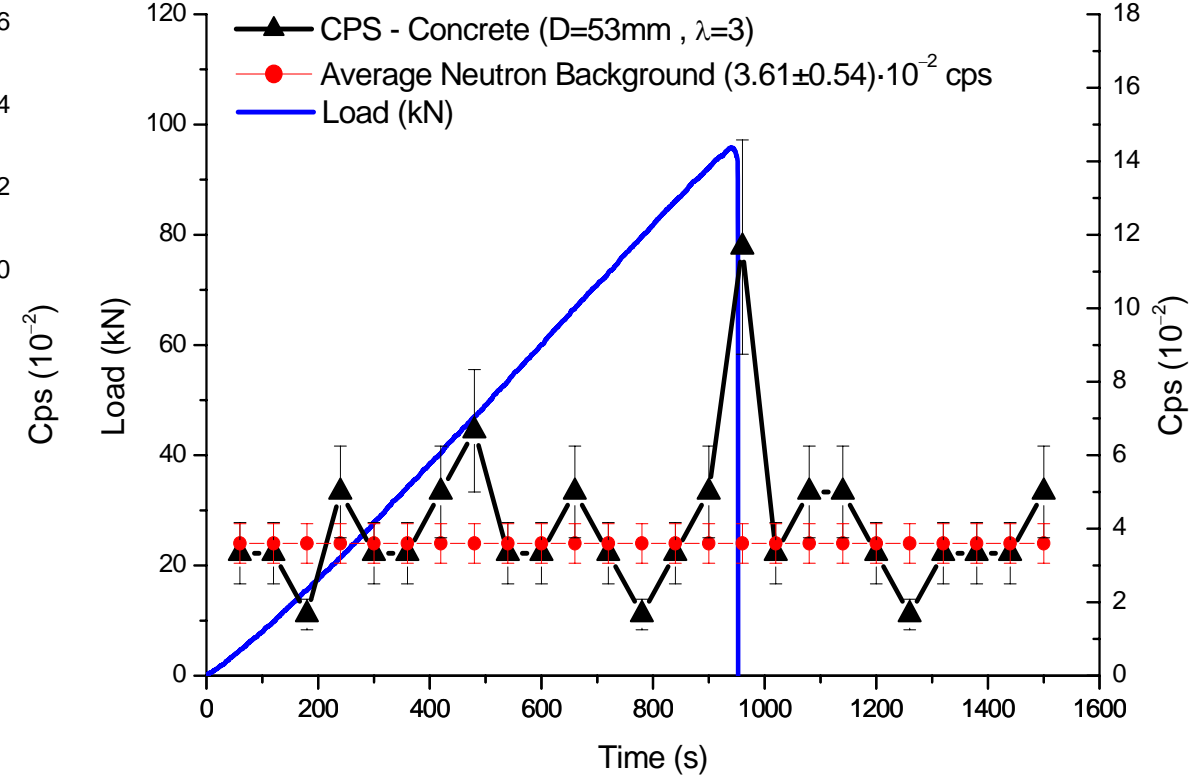
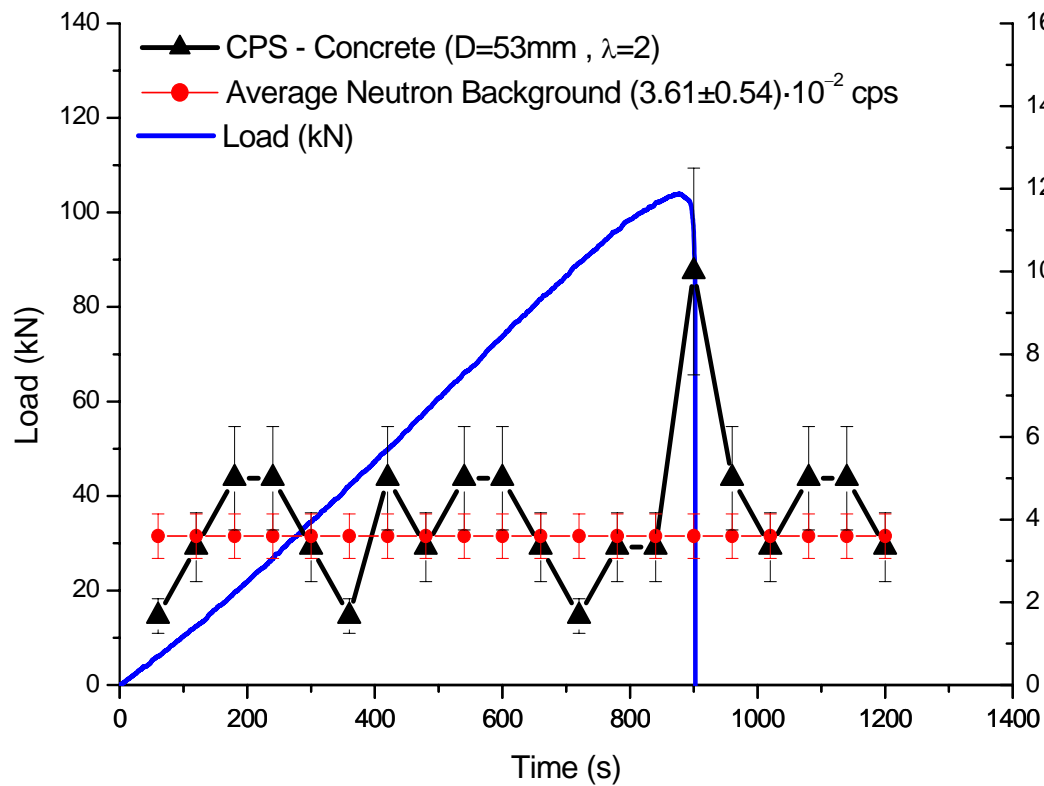




Load vs. time and cps curve for C1 test specimen in concrete.

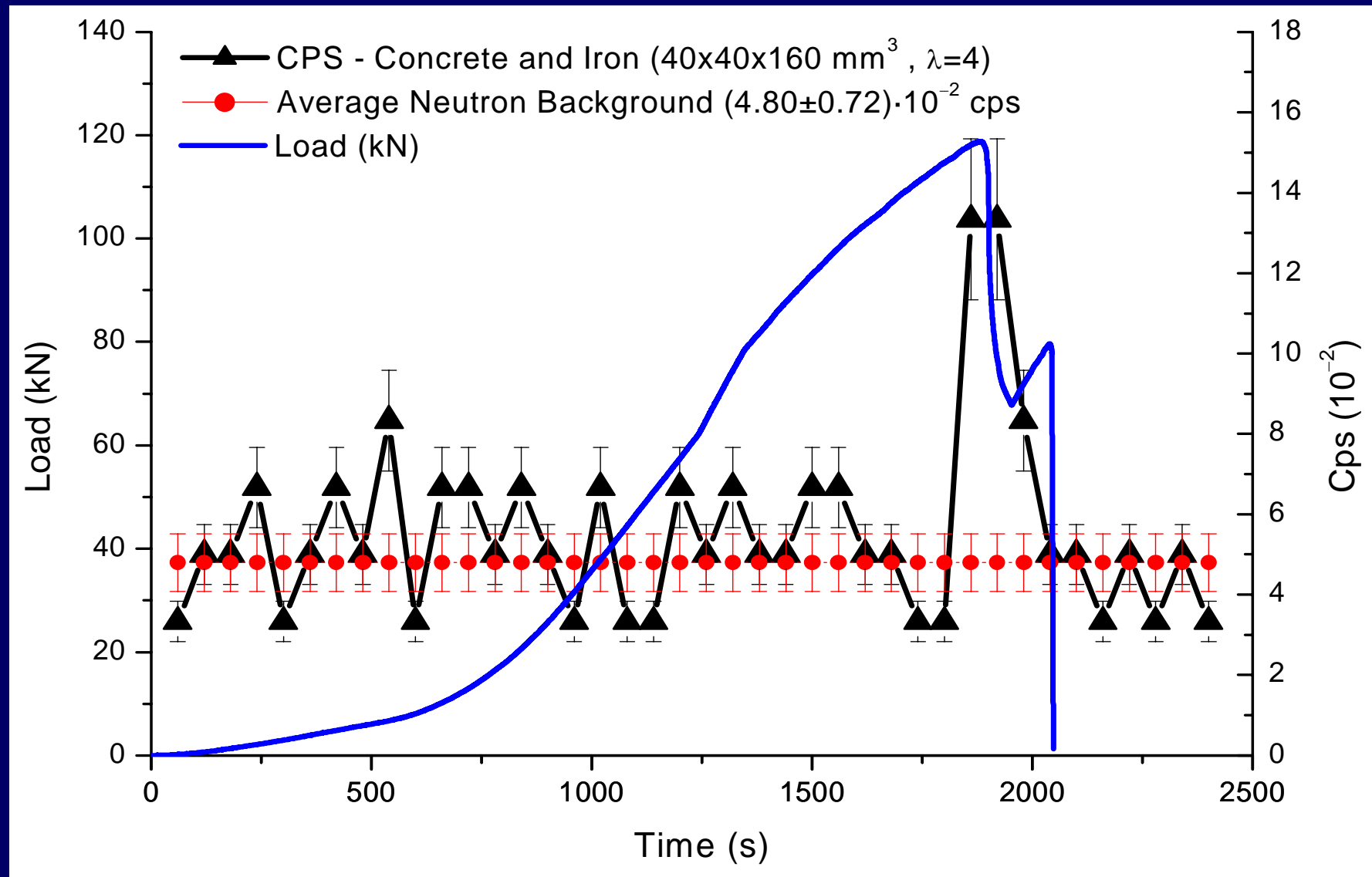


Load vs. time and cps curve for C2 test specimen in concrete.



Load vs. time and cps curve for C3 test specimen in concrete.

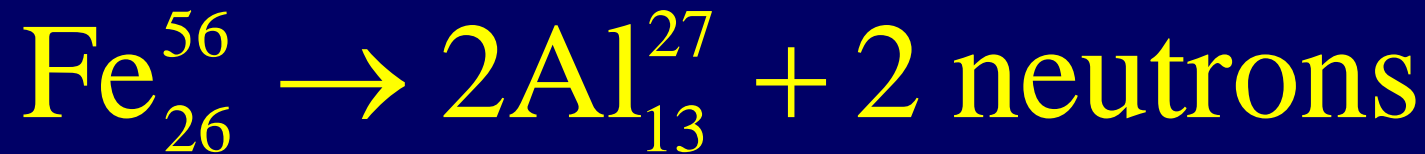
Load vs. time and cps curve for C4 test specimen in concrete.



Load vs. time and cps curve for C5 test specimen in concrete
 (10% iron content addition)

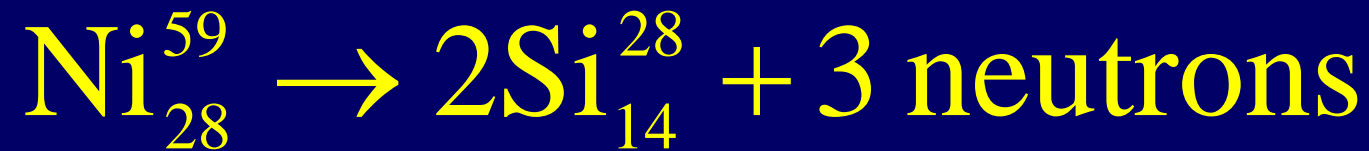
EVOLUTION OF METAL ABUNDANCES IN THE EARTH CRUST

- Based on the appearance after the experiments of aluminium atoms and the disappearance of iron atoms, our conjecture is that the following nucleolysis or piezonuclear “fission” reaction could have occurred:

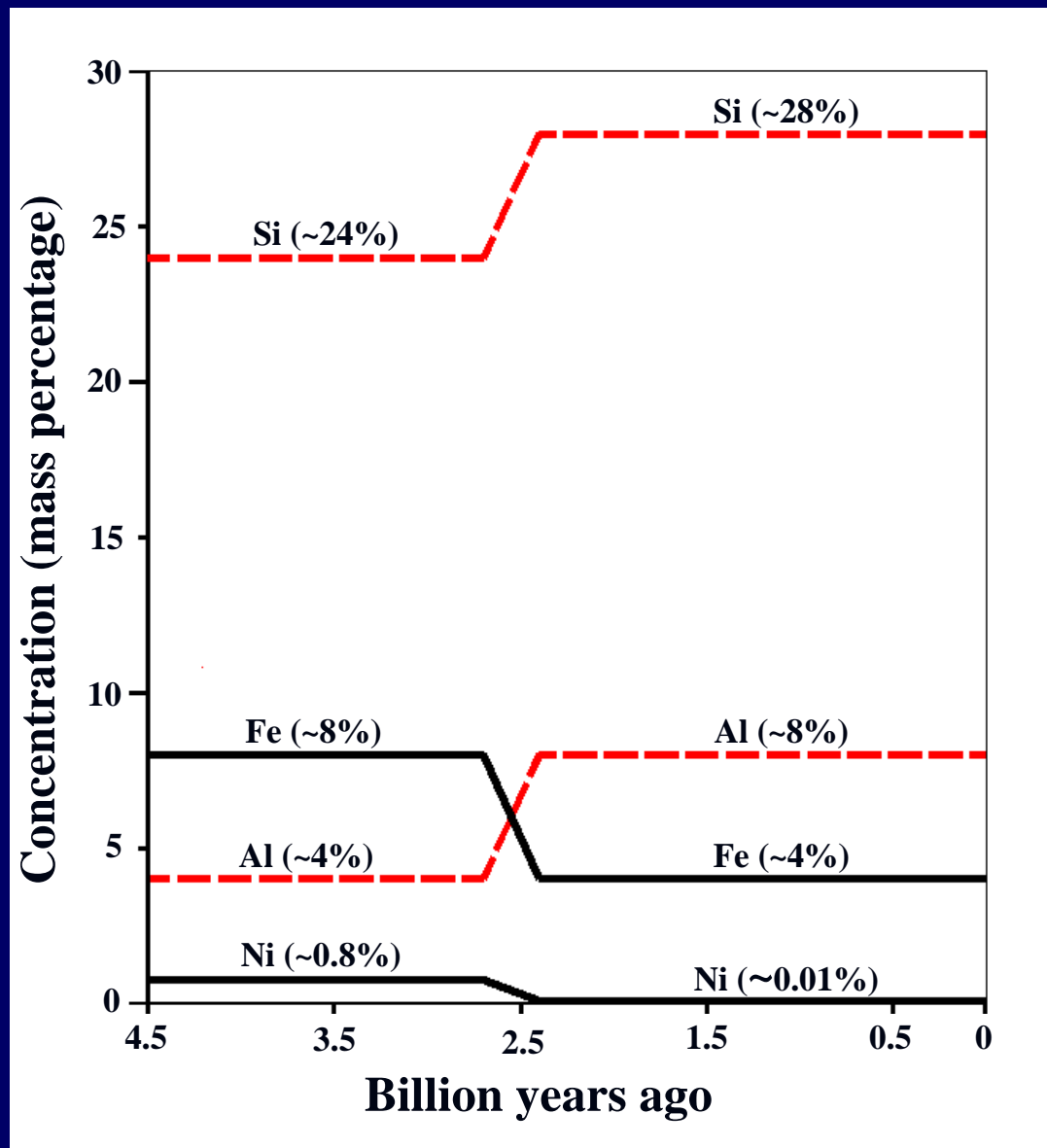


- The present natural abundance of aluminum (~8% in the Earth crust), which is less favoured than iron from a nuclear point of view, is possibly due to the above piezonuclear fission reaction.
- This reaction –less infrequent than we could think– would be activated where the environment conditions (pressure and temperature) are particularly severe, and mechanical phenomena of fracture, crushing, fragmentation, comminution, erosion, friction, etc., may occur.

- If we consider the evolution of the percentages of the most abundant elements in the Earth crust during the last 4 billion years, we realize that iron and nickel have drastically diminished, whereas aluminum and silicon have as much increased:



- It is also interesting to realize that such increases have developed mainly in the tectonic regions, where frictional phenomena between the continental plates occurred.
- Many other clues and quantitative data could be presented in favour of the piezonuclear fission reactions, and this will be the subject of a next publication.



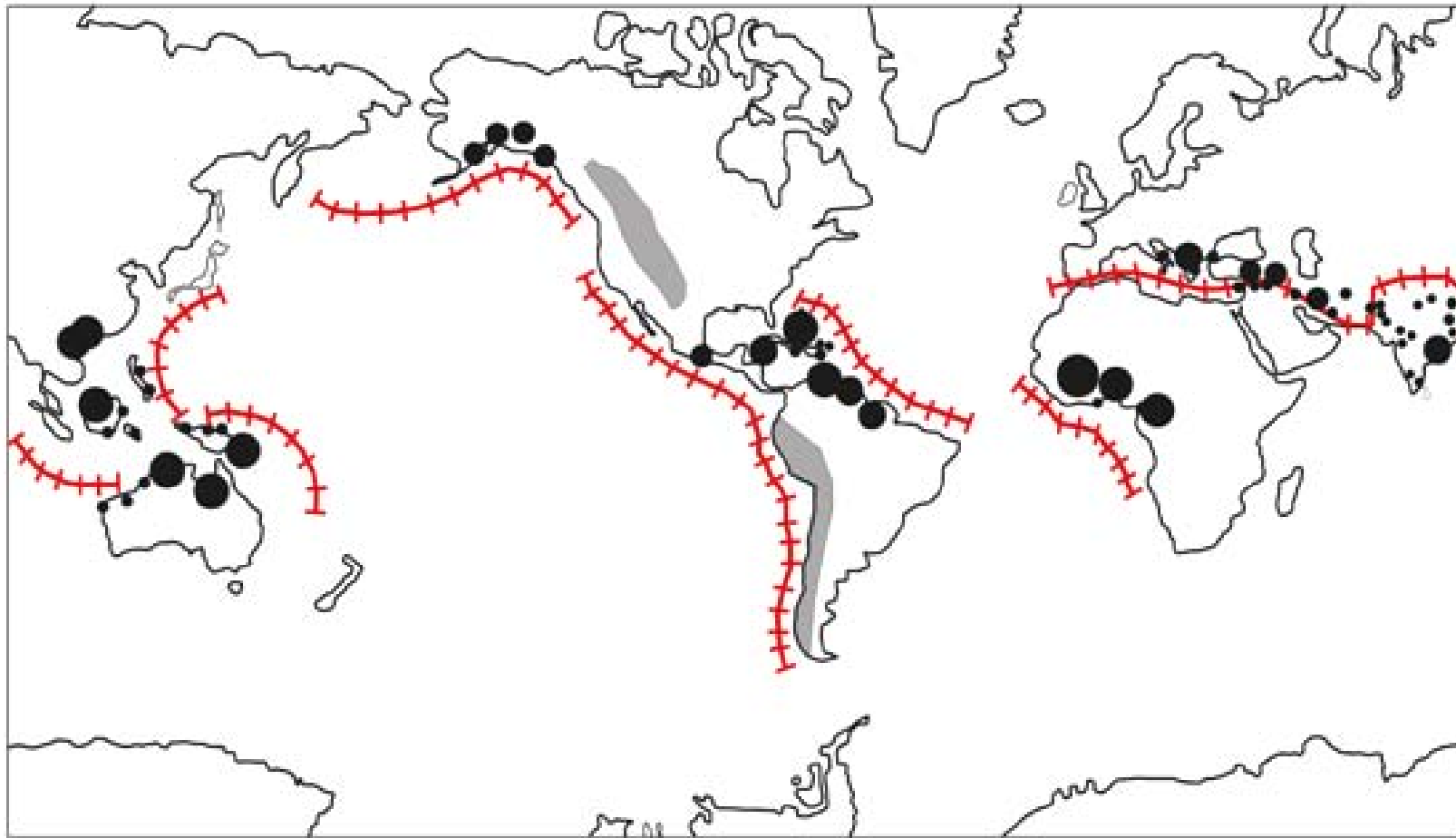
- (*) Favero G. & Jobstraibizer P. The distribution of aluminium in the Earth: From cosmogenesis to Sial evolution, *Coord.Chem. Rev.*, 1996, Vol. 149, 467–400.
- (**) Konhauser, K O. et al., Oceanic nickel depletion and a methanogen famine before the Great Oxidation Event, *Nature*, 9 April, 2009, Vol. 458, 750–754.
- (***) Anbar A. D. Elements and Evolution, *Science*, 5 December, 2008, Vol. 322, 1481–1482.



Iron reservoirs
▲ More than 40 Mt/year
▲ from 0 to 40 Mt/year

(*) World Iron Ore producers. Available at <http://www.mapsofworld.com/minerals/world-iron-ore-producers.html>.

(**) World Mineral Resources Map. Available at <http://www.mapsofworld.com/world-mineral-map.html>.



Aluminum reservoirs

- More than 10 Mt/year
- from 5 to 10 Mt/year
- from 1 to 5 Mt/year
- from 0.5 to 1 Mt/year



Subduction lines and tectonic plate trenches



Large Andesitic formations (the Rocky Mountains and the Andes)

(*) World Iron Ore producers. Available at <http://www.mapsofworld.com/minerals/world-iron-ore-producers.html>.

(**) World Mineral Resources Map. Available at <http://www.mapsofworld.com/world-mineral-map.html>.